Rapid Dry Exfoliation Method for Tuneable Production of Molybdenum Disulphide Quantum Dots or Large Micron-Dimension Sheets

A thesis submitted in fulfilment of the requirements for the degree of Master of Engineering

Mustafa Adel Ali ElSaid ElSaid Ahmed
M. Sc. (Biotechnology)
School of Sciences and Engineering, American University in Cairo
B. Sc. (Pharmaceutical Sciences)
Faculty of Pharmacy, Alexandria University

School of Engineering
College of Science, Health and Engineering
RMIT University
January 2019

Rapid Dry Exfoliation Method for Tuneable Production of Molybdenum Disulphide Quantum Dots or Large Micron-Dimension Sheets

Mustafa Adel Ali ElSaid ElSaid Ahmed

(Master of Engineering)

2019

RMIT University

Abstract of Thesis

Two-dimensional (2D) materials offer outstanding mechanical, electronic and optical properties that enabled considerable developments in a variety of applications. As such, the synthesis methods for 2D materials have gained much research interest. The preparation and synthesis of 2D materials play a significant role in its quality, hence its properties and suitability for any application. Furthermore, the cost-effective, fast, large-scale industrial production has been always a top priority and a pivotal key to the success of any application employing 2D materials. The move towards rapid large production, however, often presents trade-offs to the quality of the final product. As such, a need arises to address the problem without compromising either quality or quantity at each other's expense.

A class of 2D materials, known as transitional metal dichalcogenides, has taken the focus of research in 2D materials in the last ten years and even more recently; due to their natural abundance and interesting properties offered, when thinned down to 2D crystals. Molybdenum disulphide (MoS_2), in particular, has been extensively researched; due to its bulk form stability at room conditions, and the well-studied stability of its thinned form, allowing better control over its use, while having promising electronic and optical applications due to a suitable a bandgap, in addition to its catalytic properties, thus was found to be of use in biosensing and energy applications as well.

Many techniques have been developed for producing 2D MoS_2, whether through bottom-up synthesis or top-down exfoliation from bulk. Through the review of synthesis techniques of 2D MoS_2, none of the present approaches gave a solution that does not compromise one aspect; dictating the use of one method over the other for each application, which are often performed on small lab scale with little potential for scaling-up. The synthesis of large micron-dimension single-layer sheets of these materials remains a challenge, especially if an alternative to the slow, expensive and complex bottom-up approaches such as chemical vapor deposition or molecular beam epitaxy is desired. The top-down conventional mechanical exfoliation tape method, which was first used by Geim and Novoselov in 2004 for isolating 2D graphene from graphite and ignited a spark for the 2D materials field, remains a golden standard for pristine quality 2D materials sheets synthesis. A simple but low yield multistep method that required a lot of skill with little potential for scaling-up, however, it is still considered the standard for high quality large sheets production; due to being one of the least invasive techniques. Other mechanical exfoliation methods have been devised to address the shortcoming of the very low yield, but they usually lacked scale-up potential and introduced the use of additives for the transfer and post processing. Another approach researched in parallel was the use of liquid solvents for exfoliation that has progressed through the years starting from the harsh chemically aided exfoliation to the less invasive ultrasonication assisted exfoliation, with a promising potential for scaling-up. The liquid exfoliation techniques had a limited success in obtaining large sheets, although not comparable to the very large sheets obtained from complex bottom-up approaches but could reach the size ranges from mechanical exfoliation tape methods but with compromises made to quality in exchange for scalability. Liquid exfoliation techniques excelled in the production of smaller quantum dots, though. They offered larger yields and better processing time with relatively less complex equipment used and less skill employed. On the other hand, the use of solvents or any additives, even after extensive post

processing, still affected the quality of the produced 2D material, hence dictating the suitability for a specific application over the other.

The objective of this work is mainly to review the current synthesis techniques for 2D materials and specifically MoS_2 as the most in use example of transitional metal dichalcogenides class of 2D materials. Then to evaluate each method advantages and highlight its drawbacks to ultimately choose a synthesis route and design a platform that addresses most of the shortcomings with little or no compromise to any aspect of the produced 2D material. A novel and a unique method to rapidly exfoliate MoS_2 is presented. Tuneability is offered to produce small nanometer-dimension quantum dots of a desired size range. Moreover, the platform flexibility allowed to produce large micron-dimension as well. Both products were predominantly monolayers to few layers and the exfoliation process was conducted in dry conditions with no use of liquids or additives. The platform employs nanometer-amplitude MHz-order surface vibrations in the form of surface acoustic waves. To produce quantum dots, the bulk material is subjected to massive surface acceleration -on the order of 10^8 m/s^2- to be repeatedly impacted, ejected and collide with miniature enclosure inner walls, in order to laterally break reducing its dimensions as well as thinned down to single or few layers. On the other hand, sheets are produced by suppressing the iterative impacts cycles through reducing the enclosure height to almost zero through the use adhesive tape in place of the miniature enclosure, which serves to fix upper layers of the bulk material while the lowermost one is subjected to a shearing force from the travelling surface acoustic wave, thus progressively thinning the material into sheets while preserving their lateral dimension. A dry stable exfoliated powder product with limited restacking problems is obtained that can stored as a stock and readily used. Depending on the intended application, further suspending it before use in an easily removable solvent such as water-ethanol binary mixture can be performed for finer size separation. The platform is applicable to larger particle size bulk material feed instead of

the used commercially available 6 μm powder for demonstration, especially if optimization towards the production of sheets rather than quantum dots is intended. Furthermore, quantum dots are produced in a fast millisecond scale process in a miniaturized platform with potential for scaling-up through massive parallelization.

In conclusion, a fast, additive-free and dry exfoliation platform is presented that potentially presents a simple yet scalable micromechanical exfoliation method towards viable commercial production of 2D transition metal dichalcogenides.

Keywords: Two Dimensional Materials – Transition Metal Dichalcogenides – Molybdenum Disulphide – Exfoliation – Surface Acoustic Waves

Declaration

I certify that except where due acknowledgement has been made, the work is that of the author alone; the work has not been submitted previously, in whole or in part, to qualify for any other academic award; the content of this thesis is the result of work which has been carried out since the official commencement date of the approved research program; any editorial work, paid or unpaid, carried out by a third party is acknowledged; and, ethics procedures and guidelines have been followed.

.....

Mustafa A. Ahmed
16th of January 2019

Acknowledgements

I would like to thank all the wonderful people who contributed to this work in different ways and made this master thesis possible. First, I would like to thank my supervisors, Prof. Leslie Yeo and Dr. Amgad Rezk, and express my deepest gratitude or giving me the chance to work on this research, their insightful comments, and providing all the support needed. A special thanks to my advisor Dr. Amgad for not only his guidance but being my friend in the times I needed one the most. I would also like to thank my sister, friend and fellow lab mate Dr. Heba Ahmed for her support and always pointing me to the right direction and not giving up on me.

I would also like to extend my deepest appreciation to the school of engineering at RMIT for providing me with scholarship support through my studies. Many thanks to RMIT facilities and helpful staff, especially MicroNano Research Facility (MNRF) and RMIT Microscopy and Microanalysis Facility (RMMF), but most of all their helpful staff and researchers.

To all my wonderful fellow lab mates at MicroNano Research Lab (MNRL) at RMIT, thank you for your company and all the help you have given me. Thanks to my friends for keeping our friendship alive continents apart. Lastly, thanks to mom and dad for their continued support and love.

Journal publication(s)

The research conducted by the author of this Master of Chemical Engineering thesis was reported in a manuscript prepared and submitted to a peer reviewed journal. In addition, contribution to related work by peers, during the course of the study, was published and listed as follows:

- **Rapid Dry Exfoliation Method for Tuneable Production of Molybdenum Disulphide Quantum Dots and Large Micron-Dimension Sheets**

  Ahmed M., Ahmed H., Rezk A. R., Yeo L. Y. Nanoscale, 11, 11626-11633, doi:10.1039/C9NR04255E (2019).

- **Increasing Exfoliation Yield in the Synthesis of MoS2 Quantum Dots for Optoelectronic and Other Applications through a Continuous Multicycle Acoustomicrofluidic Approach**

  Marqus S., Ahmed H., **Ahmed M.**, XU C., Rezk A. R., Yeo L. Y. ACS Applied Nano Materials 1, 2503-2508, doi:10.1021/acsanm.8b00559 (2018).

Table of Contents

List of Figures

Abbreviations

0D	zero dimensional
1D	one dimensional
2D	two dimensional
3D	three dimensional
AFM	atomic force microscopy
BAW	bulk acoustic waves
CVD	chemical vapor deposition
FBAR	film bulk acoustic resonator
HER	hydrogen evolution reaction
HR-TEM	high resolution – transmission electron microscopy
IDTs	interdigitated transducer
Li^+	lithium ion
$LiNbO_3$	lithium niobite
M	metal atom
Mo	molybdenum
MHz	megahertz
MoS_2	molybdenum disulphide
MoO_3	molybdenum trioxide
NMP	N-Methyl-2-Pyrrolidone
PL	photoluminescence
PVD	physical vapor deposition
QCM	quartz crystal microbalance
QDs	quantum dots
RF	radio frequency
S	sulphur
SAW	surface acoustic waves
SPUDT	single phase uni-directional transducers
SSAW	standing surface acoustic waves
TMDs	transition metal dichalcogenides

UV	ultra violet
Vis	visible
X	chalcogen atom
XRD	x-ray diffraction
XPS	x-ray photoelectron spectroscopy

Chapter 1

1.1 Motivations

Microfluidics mainly using Surface Acoustic Waves (SAW) has emerged as a field of high importance that promises miniaturization and automation of many common processes. The field offered not only miniaturization of lab processes but the possibility of their integration in a compact design thus giving a lab on a chip with superior performance to other actuation techniques. The established body of knowledge in fluid physics, miniaturization on chips for electronics applications and previous applications of acoustic devices in communications and sensing all provided a stepping stage for the field of acoustically driven microfluidics [1-12]. On the other hand, relatively little work has been done on the coupling the acoustic waves to solid phase particles and their actuation [13-16]; therefore, a need to expand knowledge in this area arises in order to attain useful applications that can benefit from both the miniaturized design of acoustic devices and dry conditions. The extension to manipulating solid phase particles is considered new and promising for many applications, especially as SAW have been recently shown to have an exfoliating action beyond the already known fluid actuation on Two-Dimensional (2D) materials dispersion in an acoustomicrofluidic setup [17, 18]. SAW devices were successfully demonstrated as a platform for the liquid phase synthesis of nanosized, i.e. Zero-Dimension (0D), Quantum Dots (QDs) from layered 2D materials that possess great use in bio-sensing,

bio-imaging and reactions catalysis among other various applications. The offering of a simple alternative technique to the currently known 2D materials synthesis approaches [19-21], with both superior speed and overall efficiency was a significant advancement. However, the conservation of the product quality by avoiding the use of a solvent or additives have been elusive. Moreover, the establishment of control over the exfoliated material lateral size and thickness left room for enhancement. Therefore, a move towards the investigation of SAW effect on 2D material in dry phase is warranted. Rapid tuneable production of high quality QDs, compatible with different uses, is expected. The elucidation of the underlying mechanism for the powder exfoliation, followed by optimization of the platform design for tuneability, and the concurrent use of different characterization techniques to uncover the nature of the exfoliated 2D material and verify the platform design; are the major steps followed in this study. Once an understanding had been established, the platform design was modified towards the production of larger micron dimension sheets of 2D materials in order to illustrate the versatility of the proposed platform, added to the mentioned advantages over other 2D materials synthesis techniques.

In this work we borrowed the aspects studied in SAW driven microfluidics and apply, where appropriate, to solid phase; in order to uncover the underlying mechanism by which the observed effect of SAW on layered 2D material particles appear in experiments. Then we moved to optimize the process and to provide a better control over the exfoliation product once a good understanding had been established. The focus of this work is using SAW on Lithium Niobate ($LiNbO_3$) substrate in order to manipulate solid phase particles on the SAW device in air medium, rather than being suspended in liquid, for the purpose of exfoliating layered 2D materials without the use of any additives or solvents. The choice of SAW, beside the small acoustic wavelength for micro scale manipulation, is due to the focus of energy on the surface of the substrate together with the extreme acceleration that can be

attained [12, 22, 23]. These desirable properties serve well the aim of exfoliating 2D materials as well as de-aggregating powders. In addition, $LiNbO_3$ substrate is well suited for such use, generally due to its high electromechanical coupling coefficient, allowing the efficient conversion of energy to SAW and in turn bulk material exfoliation [24-26].

In conclusion, the need to expand knowledge for SAW interaction with solid phase particles does not only arise from the relative scarcity of research work on this area, but the immediate beneficial applications it offers. The need to expand knowledge in this area arises in order to attain useful applications that can benefit from both miniaturized design of acoustic devices and dry conditions, specifically offering a compact, rapid, solvent and additive free platform for the production of 2D material. Furthermore, the simple and miniaturized design of SAW devices is highly beneficial in particle size reduction and de-aggregation processes on different scales: it is well suited for incorporation in dry powder inhalation drug delivery devices, or scaled to lab equipment, or larger industrial scale.

1.2 Objectives

This study is constructed around addressing the following research questions:

1 **How** can the application of surface acoustic waves affect layered bulk two-dimensional materials in solid phase? And **How** can a surface acoustic waves device be applied to two-dimensional materials powder for the purpose of particle size reduction and exfoliation? And **How** does it compare to alternative exfoliation techniques?

2 **Can** the proposed technique for exfoliation cater for both micron-size two-dimensional material sheets or nanometer-sized quantum dots production through simple change in the design configuration?

3 **What** is are optimum parameters that attains exfoliation in an ultrafast manner, a good

yield and giving a tuneable product?

Considering the aforementioned identified research gaps, in the previous section of this chapter, and the proposed research questions here, this research aims to address them in order to achieve the following:

1 Review the current body of knowledge throughout the duration of the study pertaining to 2D materials synthesis techniques and actuation of solid phase particles on acoustic devices.

2 Compare the proposed approach to the current alternative techniques in order to highlight the feasibility of an impactful application based on such work.

3 Demonstrate the effect of SAW on bulk 2D materials in dry conditions through manipulating different variables at a time; in order to establish a relation to each one and help uncover the underlying mechanism of the exfoliation process.

4 Establish an adequate control on the effect of SAW on powders; in order to achieve tuneability of the particle size reduction process of 2D materials towards either thinning to monolayers or reducing the lateral size.

5 Design a platform for solvent- and additive-free exfoliation of 2D materials, thus preserving the quality. The platform features the production of both of 2D sheets or 0D quantum dots, as well as tuneability to the thickness and lateral size of the exfoliated product. In addition, the low cost, the rapid processing time and the miniature chip-scale form all allow scaling-up production through massive parallelization.

1.3 Thesis Organization

The work towards achieving the objectives of this research, outlined above, is organized

into four chapters in this thesis. The first and current chapter identifies the research gap, formulates the research question, and outlines the objectives of this work.

Chapter two gives a brief overview of the current body of knowledge from literature regarding the different elements used in our rapid dry exfoliation of MoS_2 platform design, as well as information on the other exfoliation techniques employed, in order to bring the identified research gaps closer to the reader's view. In addition; throughout the 2D material synthesis methods review, a comparison is drawn between each of the discussed exfoliation techniques and our platform to further emphasize the significance of this work and the addition made to the field of study.

In chapter three, the experiment design and the observed results are presented. Beginning with the proposed platform using focused Single-Phase UniDirectional Transducer (SPUDT) on a miniature $LiNbO_3$ chip to generate a travelling SAW along the piezoelectric substrate surface. Two variants of the setup are made to cater for the production of either nano-sized QDs or micron-sized sheets from layered 2D MoS_2 material. The first miniature enclosure design on the piezoelectric surface using glass cover and side walls as spacers for setting height is designed to produce QDs. The second use of thermal adhesive tape to confine the raw 2D material in asymptotic zero-height-limit for the purpose of producing micron-sized sheets. In the effort to elucidate the underlying mechanism and subsequent establishment of control over the exfoliation process, different variables were examined: exposure time, applied surface acoustic waves power, closed chamber volume, and bulk powder feed initial load. Different characterization techniques were used to guide the design and verify the progress made:

1. Hi-speed camera to show the de-aggregation of particles in action as well as their breakup in an ejection–collision–settling cycle in short millisecond duration of SAW

exposure.

2. Atomic Force Microscopy (AFM) to show the exfoliated 2D material Three-Dimensional (3D) topography for either the produced QDs or sheets and provide representative samples for particles' thickness and size distributions.

3. UV/Vis spectrophotometer in Absorbance (Ab) and PhotoLuminescence (PL) modes for the detection of exfoliation signature of two-dimensional materials and calculation of yield.

4. High Resolution–Transmission Electron Microscopy (HR-TEM) and diffraction pattern to confirm the crystallinity of the exfoliated material through the observation of two-dimensional mesh of atoms and calculation of d-spacing. Energy-dispersive X-ray spectroscopy (EDX) is further performed with TEM for elemental analysis; to verify the chemical state of the exfoliated product and preclude possible oxidation in MoS_2 during synthesis.

5. Powder X-Ray Diffraction (XRD) to show the signature of exfoliated material as compared to bulk counterpart and the crystal phase of the produced material.

6. Raman spectroscopy to further verify the nature of the exfoliated material -and preclude possible oxidation process in MoS_2 nanosheets- and show the efficiency of the process in thinning the 2D material to very few or monolayers.

Chapter three continues to present the results, which are discussed in detail and each of the performed experiments is tied to the major theme outlined below:

1. On application of surface acoustic waves of a suitable frequency and power to dry powder of a known density and mean particle size placed directly on piezoelectric substrate in air, ejection into the air medium was expected due to impact with the

surface vibrating in a perpendicular manner at an extreme acceleration (*Hi-speed camera*).

2. Particles are expected to show de-aggregation as well as opposing agglomeration in air medium and particularly on redepositing back on the device surface at nodal regions of standing surface acoustic waves on the piezoelectric substrate, which was counteracted by ensuring that travelling SAW is generated instead using SPUDT design (*Hi-speed camera*).

3. A breakup of the particles was expected, especially two-dimensional materials with interlayers held only by weak van der Waals forces, during the ejection. The magnitude impact force applied suggests not only the interlayer weak forces are broken but the stronger intralayer forces thus reducing lateral size i.e. the 2D material is both thinned to monolayers and lateral size cleaved to produce QDs (*AFM, UV/Vis PL, HR-TEM, Powder XRD*). On suppressing the ejection and impact cycle in asymptotic zero-height-limit, only the shear component of the travelling SAW was expected to slide the downmost layer in the bulk material stack, thus preserving the lateral size and producing sheets (*AFM, HR-TEM, Powder XRD, Raman spectroscopy*).

4. The miniature enclosure design of a relatively small height is expected to maximize the powder particles breakup due to increased instances of impact, which was observed to be the major force acting against the integrity of particles for size reduction as well as van der Waals forces holding aggregates and 2D materials in stacks (*Theoretical calculation derived from experimental data*).

5. The asymptotic zero-height-limit setup, in which the bulk powder feedstock is confined under adhesive tape, progressively delaminated the bulk 2D material into large micron-sized sheets by the shearing component parallel to the travelling direction of

propagation along the substrate surface.

6. The extreme acceleration on the piezoelectric surface by surface acoustic waves greatly increased the force of impact; therefore, the required exposure time to observe a significant exfoliation in bulk two-dimensional materials / particle size reduction and de-aggregation of powder was greatly reduced to ultra-fast milliseconds and a trend of increase in quantum yield was observed with increased exposure time (*AFM, UV/Vis PL*). In addition, the applied power for the exfoliation process followed the same positive trend as that observed with increased exposure time.

7. In asymptotic zero-height-limit setup, the exfoliation process showed rapid exfoliation, albeit being relatively longer in SAW exposure requirement and relatively less in the observed yield than the miniature enclosure setup. The suppression of impact and ejection cycles by design limited the role of either time or applied SAW power to increasing the delivered energy for the exfoliation process only, while not altering its chemical nature (*UV/Vis Ab*, *TEM-EDX*).

Finally, chapter four will discuss the overall conclusion of this research and present the possible future direction that can build upon this work.

1.4 References

1. Campbell, C., *Surface Acoustic Wave Devices and Their Signal Processing Applications.* The Journal of the Acoustical Society of America, 1991. **89**(3): p. 1479-1480.
2. Baudoin, M., et al., *Low power sessile droplets actuation via modulated surface acoustic waves.* Applied Physics Letters, 2012. **100**(15): p. 154102.
3. Brunet, P., et al., *Droplet displacements and oscillations induced by ultrasonic surface acoustic waves: A quantitative study.* Physical Review E, 2010. **81**(3): p. 036315.
4. Bussonnière, A., et al., *Dynamics of sessile and pendant drops excited by surface acoustic waves: Gravity effects and correlation between oscillatory and translational motions.* Physical Review E, 2016. **93**(5): p. 053106.

5. Ding, X., et al., *Surface acoustic wave microfluidics.* Lab on a Chip, 2013. **13**(18): p. 3626-3649.
6. Dung Luong, T. and N. Trung Nguyen, *Surface Acoustic Wave Driven Microfluidics - A Review.* Micro and Nanosystems, 2010. **2**(3): p. 217-225.
7. Fu, Y.Q., et al., *Advances in piezoelectric thin films for acoustic biosensors, acoustofluidics and lab-on-chip applications.* Progress in Materials Science, 2017. **89**: p. 31-91.
8. Luo, J., Y.Q. Fu, and W. Milne, *Acoustic wave based microfluidics and lab-on-a-chip*, in *Modeling and Measurement Methods for Acoustic Waves and for Acoustic Microdevices*. 2013, InTech.
9. Renaudin, A., et al., *Creeping, walking and jumping drop.* Physics of Fluids, 2007. **19**(9): p. 091111.
10. Shilton, R.J., et al., *Rotational microfluidic motor for on-chip microcentrifugation.* Applied Physics Letters, 2011. **98**(25): p. 254103.
11. Wixforth, A., et al., *Acoustic manipulation of small droplets.* Analytical and bioanalytical chemistry, 2004. **379**(7-8): p. 982-991.
12. Yeo, L.Y. and J.R. Friend, *Surface Acoustic Wave Microfluidics.* Annual Review of Fluid Mechanics, 2014. **46**(1): p. 379-406.
13. Guo, F., et al., *Three-dimensional manipulation of single cells using surface acoustic waves.* Proceedings of the National Academy of Sciences, 2016. **113**(6): p. 1522.
14. Miansari, M., et al., *Vibration-Induced Deagglomeration and Shear-Induced Alignment of Carbon Nanotubes in Air.* Advanced Functional Materials, 2014. **25**(7): p. 1014-1023.
15. Sakano, K., M.K. Kurosawa, and T. Shigematsu, *Driving Characteristics of a Surface Acoustic Wave Motor using a Flat-Plane Slider.* Advanced Robotics, 2010. **24**(10): p. 1407-1421.
16. Tan, M.K., J.R. Friend, and L.Y. Yeo, *Direct visualization of surface acoustic waves along substrates using smoke particles.* Applied Physics Letters, 2007. **91**(22): p. 224101.
17. Ahmed, H., et al., *Ultrafast Acoustofluidic Exfoliation of Stratified Crystals.* Advanced Materials, 2018. **30**(20): p. 1704756.
18. Marqus, S., et al., *Increasing Exfoliation Yield in the Synthesis of MoS_2 Quantum Dots for Optoelectronic and Other Applications through a Continuous Multicycle Acoustomicrofluidic Approach.* ACS Applied Nano Materials, 2018. **1**(6): p. 2503-2508.
19. Brent, J.R., N. Savjani, and P. O'Brien, *Synthetic approaches to two-dimensional transition metal dichalcogenide nanosheets.* Progress in Materials Science, 2017. **89**: p. 411-478.
20. Gupta, A., T. Sakthivel, and S. Seal, *Recent development in 2D materials beyond graphene.* Progress in Materials Science, 2015. **73**: p. 44-126.
21. Nicolosi, V., et al., *Liquid Exfoliation of Layered Materials.* Science, 2013. **340**(6139).
22. Yeo, L.Y. and J.R. Friend, *Ultrafast microfluidics using surface acoustic waves.* Biomicrofluidics, 2009. **3**(1): p. 012002.
23. Friend, J. and L.Y. Yeo, *Microscale acoustofluidics: Microfluidics driven via acoustics and ultrasonics.* Reviews of Modern Physics, 2011. **83**(2): p. 647-704.
24. Yamada, T., N. Niizeki, and H. Toyoda, *Piezoelectric and Elastic Properties of Lithium Niobate Single Crystals.* Japanese Journal of Applied Physics, 1967. **6**(2): p. 151-155.
25. Fukuda, T., V.I. Chani, and K. Shimamura, *Lithium Niobate, Lithium Borate, and Lithium Tantalate for NLO*, in *Encyclopedia of Materials: Science and Technology*, K.H.J. Buschow, et al., Editors. 2001, Elsevier: Oxford. p. 4603-4609.
26. Wong, K.-K., *Properties of lithium niobate*. 2002: IET.

Chapter 2

2.1 Literature Review

2.1.1 A Brief Overview of Acoustics in Microfluidics and Sensing

The acoustic waves are generated by applying a Radio Frequency (RF) on a PiezoElectric (PE) material, usually through an InterDigitated Transducer (IDT) photolithographed on the PE substrate. The IDT design determines the frequency and the mode of the generated acoustic wave [1, 2], which in turn determines the choice of the piezoelectric material for the chip best suited for the intended use. The IDT design should be optimized as well for the intended application, as the generated wave can be generally used for actuation of fluid residing on the substrate whether lying directly on the surface, or actuated through a coupling layer, the fluid can also be lying on the surface confined by its surface tension, or in an etched or bonded microchannel. For sensing purpose, the most common setup makes use of the generated wave when received back through another IDT to detect changes in the signal resulting from coupling of the wave to the sample on the substrate [2, 3].

Different modes of acoustics waves are used (Figure 2.1), ranging from Bulk Acoustic Waves (BAW) travelling inside the material perpendicular to the surface, to Surface Acoustic Waves (SAW) traveling along the surface. SAW further operates in two modes: either as Rayleigh wave with longitudinal component confined to the surface and a vertical

shear component, or shear wave that is horizontal in-plane of the surface. The former Rayleigh mode can operate in a thin substrate that is in the order of the acoustic wave length, giving rise to Lamb waves that cause only flexures. The latter shear horizontal mode is usually used for Love waves that are also known as horizontally polarized surface skimming bulk waves through a thin guide layer deposited on the PE substrate and having a lower shear acoustic velocity [2, 4].

Figure 2.1. Different modes of acoustic waves (a) Quartz Crystal Microbalance (QCM) (b) Rayleigh SAW (c) Lamb Waves (d) Shear horizontal SAW (e) Love Mode Wave (f) Film Bulk Acoustic Resonator (FBAR), where (b-e) are SAW types, while (a) and (f) are BAW types. Adapted from [2].

The use of acoustic waves for sensing predated the emergence of acoustics in microfluidics and continues to be an active research area due to their simple operation, high sensitivity, small size, fast response and low cost. It is commonly focused on biosensing and

chemical sensing mostly in liquid medium. Chemical sensing has been shown to have application that extend to sensing in gaseous phase. SAW based sensing is situated, according to sensing sensitivity, in mid area between Quartz Crystal Microbalance (QCM) and Film Bulk Acoustic Resonator (FBAR). Both QCM and FBAR operate by BAW, the former being quartz crystal sandwiched between two electrodes and operates at lower frequency due to limitation on the crystal thinness, while the latter employs sub micrometer PE film thus operating at higher frequencies up to few GHz [2, 4]. Sensors based on SAW Rayleigh mode are more suited for sensing in gases rather than fluids as coupling to longitudinal waves in liquid medium causes loss of signal. SAW shear horizontal mode is more suited for sensing in liquids [3]. However, the coupling effect is of great use in microfluidics. The SAW induced streaming and build-up of acoustic radiation pressure results in internal streaming in droplet or liquid in confined channel, and with increasing SAW power different effects are observed that are made of use in manipulating fluids on micro scale (Figure 2.2) [5, 6].

<Image removed due to copyright restrictions>

Figure 2.2. Acoustic streaming in (a) droplet (b) confined channel. (c) **The changing effect on fluid with increasing power loads** (1) mixing (2) motion (3) jetting (4) atomization. Adapted from [6].

At low power droplet vibration and internal streaming allow for droplet mixing, concentration [7] and droplet heating [8] as well as patterning at nodes using standing SAW (SSAW) waves that arise from interference of two opposing SAW waves, where one is usually a reflection of the other [5, 9]. SSAW finds another interesting application as acoustic tweezers that can manipulate *solid phase* particles in three dimensions in air [10]. Particles in liquid flow can also be separated by SAW or SSAW [5, 9]. Actuation is made possible at higher power can be manifested in drop translation or transport in microchannel [6, 9]. Microcentrifugation is another application made possible by apply relatively higher SAW power [5, 9]. At increased SAW power droplet jetting or further atomization into aerosol droplet is accomplished, which finds use as an application in medicine and drug delivery [4, 9].

2.1.2 Focus on SAW Devices Suitable for Manipulating Solid Phase Particles

Similar to microfluidics, the maximized coupling of acoustic energy to solid phase particle from PE substrate, although through different underlying mechanism [11, 12] makes SAW in Rayleigh mode a very good candidate for solid phase particles manipulation.

<Image removed due to copyright restrictions>

Figure 2.3. Two superimposed SSAW setup for 3D acoustic tweezers (a) particle entrapped in node (b) simulation results for mapping of acoustic field around entrapped particle. Adapted from [10].

From the many of microfluidic applications of SAW and SSAW briefly mentioned earlier, some can extend to solid particles settled on PE substrate in air especially acoustic tweezers that offered control in z dimension through the input power and phase change SSAW component waves for movement in x-y plane (Figure 2.3) [10].

The current work in literature studying the effect of SAW on solid phase particles is limited. Early work has been done on manipulating acoustic waves to design a microscale motor via sliding a silicon sheet by friction with a traveling Rayleigh wave contact point on PE substrate [13, 14]. The friction motor drive concept (Figure 2.4), originally intended for robotics applications, was used as a base in this study for our design aimed at the exfoliation of bulk 2D MoS_2 to micron-sized sheets in dry conditions. Powder particles transport by SAW has been studied as well and showed the feasibility of control over microscale particles and dispensing in milligrams. Moreover, the study made use of unconventional IDTs orientations, which are usually situated to generate SAW along PE substrate crystal plane for a maximum electromechanical coupling coefficient, and showed the resulting different behaviors in powder transport [15].

<Image removed due to copyright restrictions>

Figure 2.4. Friction drive concept originally used in robotics and makes use of the shear component of travelling SAW. Adapted from [14].

Moving to the manipulation of rather smaller particles and for the purpose of visualizing acoustic waves using smoke particles (Figure 2.5), Tan et al. modelled the possible underlying mechanism by which SAW interacts with solid phase particles [12]. Although the particles in the study were suspended in air, it accounted for radiation pressure, drag by acoustic streaming and dominant force of mechanical impact with PE substrate on ejection. The study also attempted to make use and explain in detail the phenomenon of particle agglomeration and offered clues on how to avoid it, as it is not desired as in this current study.

<Image removed due to copyright restrictions>

Figure 2.5. The interaction of SAW with solid phase smoke particles (a) Illustration of smoke particles agglomeration b) Impact force, drag from acoustic streaming and radiation pressure causing lift of particles and the latter two translating it to nodal regions before settling. Adapted from [12].

Miansari et al. showed the possibility of detangling and aligning One-Dimension (1D) Multi Walled Carbon NanoTubes (MWCNTs) in air (Figure 2.6), thus circumventing the

substantial processing with liquid phase detangling methods, use of surfactants, and chemical functionalization for the purpose of detangling. The use of SAW was also shown to be superior to wet ultrasonication and ball milling that damage the nanostructure. The study further accounted for the electric field generated by PE substrate [11]. The study also pointed out the relation of impact force with carbon nanotube bundle radius and increased van der Waals cohesive force. At such small scale repeated attenuated impacts and weathering are expected to play a role in observed exfoliation or particle size reduction.

<Image removed due to copyright restrictions>

Figure 2.6. The interaction of SAW with multi walled carbon nano-tubes (MWCNTs) in air. Field emission gun scanning electron microscopy (FEG-SEM) images (a) Small bundle of carbon nano-tubes generated purely via impact force of SAW by grounding electric field through a layer of gold atop the $LiNbO_3$ substrate (b) Individual carbon nano-tubes begin to appear on the periphery using non-grounded substrate via mechanical force

and Columbic fission (c) More detangling down to individual carbon nano-tubes with increased SAW exposure. Adapted from [11].

2.1.3 Layered MoS_2 as 2D Material

The early spark in the field on 2D materials started with the isolation and characterization of graphene by Geim and Novoselov in 2004, an atomically thin sheet of hexagonal units made of carbon atoms [16-18]. The novel 2D material offered interesting chemical, thermal, mechanical, electronic and optical properties and quantum size effects different from its bulk form, which opened the door to various applications. Capitalizing on this advance, many graphene analogues became of high interest and they were found to be even superior alternatives for many applications where they possess better suited properties [19, 20]. Transition Metal Dichalcogenides (TMDs) are one class of such 2D materials, with molybdenum disulphide (MoS_2) in particular having been the focus of research in 2D material in the last ten years and even more recently [19, 21, 22]. TMDs are not one layer of atoms like graphene. A monolayer of TMDs is structured as two planes of hexagonal units made of chalcogen atoms (X) sandwiching a plane of transition metal atoms (M) thus having the formula MX_2 (Figure 2.7) [19, 22]. These layers are held together by weak van der Waals forces when in the bulk form thus having an interlayer spacing.

<Image removed due to copyright restrictions>

Figure 2.7. Atomic structure of MoS_2. Showing monolayers of transitional metal sandwiched between two planes chalcogens (X) atoms, and interlayer spacing of 6.5 Å. Adapted from [23].

Originally, MoS_2 has been used in industry as a dry lubricant; but since the discovery of its 2D form, it has been the focus of 2D materials research and extensively studied due to its natural abundance and bulk form stability in room conditions. The well-studied stability of its thinned form, where the exposed edge sites of monolayers and few layers are susceptible to oxidation at room conditions that spreads to the surface in a reaction accelerated by photons [24, 25], allows better control over its use in 2D crystal form. Furthermore, it acquires interesting size dependent properties once it reaches 2D domain, such as outstanding mechanical, electronic and optical properties that enabled considerable developments in a variety of applications [26-30], in addition to, its catalytic properties [31-33], thus it was found to be of great use in sensing [29, 34] and energy applications [35-37] as well.

Layered 2D MoS_2 possess band structure that is dependent on the lack of interlayer forces, hence the change in its thickness towards atomically thin monolayers [38, 39] is essential to its application in electronics as it transitions from indirect to direct bandgap [36]. Graphene, on the other hand, is locked into metallic properties due to the array of sp^2 sigma bonded carbon atoms in the graphene monolayer, thus limited in having zero band gap unless extensively engineered [16, 17] making it less than ideal as a semiconductor. MoS_2 has been employed heavily in many applications, rather than graphene, ranging from optoelectronics, photocatalysis, energy storage, photonics, and biosensing, among others [19, 40]. Other reasons for the preference of ultrathin MoS_2 crystals are having chemical activity at reactive edge sites, as well as different thermal and mechanical properties from

its bulk counterpart in a manner similar, if not superior, to graphene.

2.1.4 Current Synthesis Methods for 2D MoS_2

In spite of the well-documented properties of 2D MoS_2 and, in general, other TMDs [26, 27, 29, 41-44], the practical adoption of these materials in commercial applications largely depends on the fabrication process by which they are synthesized. In particular, the lateral dimension of exfoliated MoS_2 can vary hugely from large micron-scale sheets to small nano-scale QDs, and their thicknesses from predominantly single to several layers. The earliest exfoliation methods involved their peeling with the aid of adhesive tape [18, 45-50], which offers a way to attain pristine micron dimension sheets down to single layer thicknesses. Nevertheless, despite its simplicity, the peeling process, in addition to being rather time-consuming, is extremely skill-dependent, therefore offering very little run-to-run reproducibility of the flake dimensions and thicknesses. As such, considerable effort has since been dedicated to the development of alternative methods to exfoliate these materials, which can be broadly categorized into either bottom-up or top-down approaches.

2.1.4.1 Bottom-up Approaches

In bottom-up approaches, monolayers or few-layers of the 2D crystal are grown on a substrate, primarily by Physical or Chemical Vapor Deposition (PVD/CVD). The co-evaporation of precursors for MoS2 such as Sulphur and molybdenum trioxide (MoO_3) gives adequately pristine large 2D crystals [51-54], however, it is often challenging to transfer the crystals from the substrate they are grown on during production onto the desired substrate [51, 55, 56]. An alternative technique involving direct sulphurization of a deposited thin metal oxide layer [55, 57-60] circumvents the need for such substrate transfer, but adds further complexity to an already slow and expensive process, in which the fabrication parameters are tightly correlated with both the substrate on which the material is

to be grown on, as well as the material itself, and thus have to be finely tuned for each fabrication procedure [40, 61, 62]. In addition, the reaction requires demanding parameters and is limited in achieving precise control over the thickness of the grown film.

2.1.4.2 Top-down Approaches

Aside from the aforementioned standard mechanical exfoliation tape method, top-down approaches, typically involve agitating a liquid suspension of the material at high speeds, either with a blender [63-65] or through ultrasonication [20, 23, 66-70], for example, to drive shearing of its bulk phase into exfoliated 2D crystals. The most prominent advantage of the approach was scalability [63-65, 69, 71], unlike tape exfoliation. The processing time, however, ranged from several to even a hundred hours, especially if the monolayer yield is to be increased [20, 65, 66, 72, 73]. Paradoxically, the longer the shearing process to acquire more crystals that are in monolayer form, the greater the tendency to break the material laterally. Consequently, the 2D crystals that are usually produced with these methods typically comprise nanosheets with lateral dimensions ranging from 30 nm to 180 nm, or QDs with lateral dimensions below 15 nm [40, 65]. As such, the production of large sub-micron or micron dimension sheets are considerably challenging with these methods. Moreover, liquid exfoliation methods usually employ solvents as intercalating agents to enhance the exfoliation process [20, 66-68, 74, 75], although their use affects the quality of the exfoliated material and often poses considerable safety hazards particularly for large scale production, given that the typical solvents that are used, such as N-Methyl-2-Pyrrolidone (NMP), tend to be volatile, flammable, corrosive and toxic. Other surfactant additives or binary solvents are often used to prevent restacking of the MoS_2 layers [69, 71], although their use is also generally known to affect product purity and characteristics such as decreased conductivity [40]. While binary solvents or thermally-controlled water as a liquid medium have been used to mitigate the effect of these additives [76, 77], though the

adsorbed solvents are known to still affect the quality of the synthesized material [40].

Other widely used liquid exfoliation techniques, for much improved yield, have used intercalating agents, with lithium ion (Li^+) as the most commonly used, that extend interlayer spacing and separate layers from the stack aided by ultrasonication or the production of gas by the intercalant [78-80]. The process involves chemical reaction [79, 81] that converts 2H crystal structure to a higher energy 1T isoform (Figure 2.9), although the matrix reverts after some time [82]. Such higher energy form together with the edge defect arising from the harsh reaction are desired for use in catalysis [31, 32, 35, 78, 83, 84], but the technique is considered to be an extreme away from the techniques aiming to preserve quality of exfoliated material and its electronic and physical properties. Although monolayers are reached at high proportions than any other synthesis method [81], the process is highly specific to the targeted TMD, in addition, the high yield is accomplished at the expense of giving rise to many defects, much reduced lateral size that is not highly controllable, hours to days of processing time, re-stacking problems, and difficult to remove and highly reactive impurities. An alternative electrochemical ion exchange avoids the use of the dangerous chemicals in the reaction such as the n-butyl lithium used for Li^+ release, however, the approach had lower yield defeating the purpose [40].

Figure 2.8. Different liquid exfoliation approaches (a) intercalation (b) ion exchange (c) ultrasonication. Adapted from [20].

Figure 2.9. Crystal phases of MoS_2 (a) stable 2H phase (b) metastable 1T phase. 2H phase possess semiconductor properties and a hexagonal honeycomb mesh under HR-TEM. 1T phase is metallic and identified by a different mesh, hence d-spacing in HR-TEM. Adapted from [41] and [19].

There have since been efforts, albeit limited, to circumvent the problems associated with liquid-phase exfoliation. More recent developments involving mechanical exfoliation

have facilitated higher yield synthesis of sheets that are several hundreds of microns in dimension and allow their transfer onto a specific substrate desired for a particular application, albeit at the expense of introducing more complexity, requiring additives that comprised more aggressive etchants additive and the lacking tunability or scalability [47]. Other approaches in mechanical exfoliation involved dry grinding and milling [85], as well as other micromechanical exfoliation processes [40], such as using sandpaper [86]. The former, however, still results in typically smaller lateral sheet sizes between 30 nm and 200 nm [85] and requires the addition of bulking and abrasive agents such as sodium chloride (NaCl), which leads to contamination of the final product and hence necessitates subsequent use of a solvent for its separation, whereas the latter is generally an unscalable and slow multiple step process that results in very low yields. Whichever the method, wet or dry, the challenge nevertheless remains in obtaining contaminant-free and pristine larger sheets with sizes beyond 200 nm in lateral dimension.

To highlight the current MoS_2 QDs production techniques specifically, bottom-up and top-down approaches are also followed. Bottom-up approach involves synthesis from chemical precursors, such as hydrothermal [87] or electrochemical [88] methods. The yield is typically low; due to difficulty in controlling all the factors in the reaction, as well as the very slow processing time. Top-down approaches usually involve mechanical exfoliation [23, 85, 89], or sonication or chemical exfoliation, as discussed earlier. Although they have an improved yield, all are liquid mediated, involving additives, and have difficulty in tuneability especially the last; as it involves applying harsh conditions. The processing time is still typically in hours scale, if not days.

Regarding dispersion stability and tendency to restack after synthesis in a liquid disperse mediums; Overtime, through random motion, the exfoliated particles collide and restack; to decrease the large specific area and excess surface energy. Particles size

distribution, concentration, temperature and dispersion medium viscosity all play a role in this inherent thermodynamic instability [90]. The move from liquid dispersion, in which the exfoliated material is usually produced, to dry powder form – post-synthesis – has been found to be an attractive solution to restacking; as particles motion becomes limited. Hence, freeze dried exfoliated powder are considered to be superior to stabilized dispersions [91], although additives are still involved.

In this work, we attempt to address the aforementioned challenges associated with bottom-up and top-down approaches by developing a *dry* (solvent- and additive-free) technique that is able to synthesize relatively large micron-dimension MoS_2 sheets, or, alternatively, smaller nanoscale QDs, with acceptable monolayer yields. In either case, a dry, stable powder of exfoliated product that is free from additives and limited restacking—a problem generally associated with exfoliation involving liquid suspensions, due to the inherent thermodynamic instability in a disperse medium as opposed to limited random motion, hence particle-particle interaction in a dry powder—is obtained. The method builds upon our recent work demonstrating the possibility of utilizing surface acoustic waves (SAWs)—nanometer amplitude electromechanical waves that propagate along the surface of a piezoelectric substrate [1, 92]—to efficiently exfoliate bulk TMDs into either monolayer or few-layer 30 nm dimension nanosheets [93] or QDs [94] through a microfluidic nebulization process. However, unlike these *liquid-phase* precedents, wherein the remarkably large substrate acceleration associated with the SAW—on the order 10^8 m/s^2 [9, 95, 96]—was exploited to drive the nebulization of a *liquid* suspension of the bulk material to induce its exfoliation, we harness this extremely potent mechanism to supply the mechanical shear and impact forces necessary to drive the exfoliation process in *dry solid phase*. We shall show, in stark contrast, that this not only allows comparably thin (monolayer to few-layers), albeit significantly larger, micron-sized MoS_2 sheets to be

produced, but also allows the tuneable possibility of synthesizing nanometre-dimension QDs—both without necessitating any liquid, including solvents and additives.

2.2 References

1. Campbell, C., *Surface Acoustic Wave Devices and Their Signal Processing Applications.* The Journal of the Acoustical Society of America, 1991. **89**(3): p. 1479-1480.
2. Fu, Y.Q., et al., *Advances in piezoelectric thin films for acoustic biosensors, acoustofluidics and lab-on-chip applications.* Progress in Materials Science, 2017. **89**: p. 31-91.
3. Devkota, J., P.R. Ohodnicki, and D.W. Greve, *SAW Sensors for Chemical Vapors and Gases.* Sensors, 2017. **17**(4): p. 801.
4. Luo, J., Y.Q. Fu, and W. Milne, *Acoustic wave based microfluidic and lab-on-chip.* 2013.
5. Ding, X., et al., *Surface acoustic wave microfluidics.* Lab on a Chip, 2013. **13**(18): p. 3626-3649.
6. Dung Luong, T. and N. Trung Nguyen, *Surface Acoustic Wave Driven Microfluidics - A Review.* Micro and Nanosystems, 2010. **2**(3): p. 217-225.
7. Shilton, R., et al., *Particle concentration and mixing in microdrops driven by focused surface acoustic waves.* Journal of Applied Physics, 2008. **104**(1): p. 014910.
8. Guttenberg, Z., et al., *Planar chip device for PCR and hybridization with surface acoustic wave pump.* Lab on a Chip, 2005. **5**(3): p. 308-317.
9. Yeo, L.Y. and J.R. Friend, *Surface Acoustic Wave Microfluidics.* Annual Review of Fluid Mechanics, 2014. **46**(1): p. 379-406.
10. Guo, F., et al., *Three-dimensional manipulation of single cells using surface acoustic waves.* Proceedings of the National Academy of Sciences, 2016. **113**(6): p. 1522.
11. Miansari, M., et al., *Vibration-Induced Deagglomeration and Shear-Induced Alignment of Carbon Nanotubes in Air.* Advanced Functional Materials, 2014. **25**(7): p. 1014-1023.
12. Tan, M.K., J.R. Friend, and L.Y. Yeo, *Direct visualization of surface acoustic waves along substrates using smoke particles.* Applied Physics Letters, 2007. **91**(22): p. 224101.
13. Kurosawa, M.K., *State-of-the-art surface acoustic wave linear motor and its future applications.* Ultrasonics, 2000. **38**(1): p. 15-19.
14. Sakano, K., M.K. Kurosawa, and T. Shigematsu, *Driving Characteristics of a Surface Acoustic Wave Motor using a Flat-Plane Slider.* Advanced Robotics, 2010. **24**(10): p. 1407-1421.
15. Saiki, T., et al., *Interdigital transducer generated surface acoustic waves suitable for powder transport.* Advanced Powder Technology, 2017. **28**(2): p. 491-498.
16. Castro Neto, A.H., et al., *The electronic properties of graphene.* Reviews of Modern Physics, 2009. **81**(1): p. 109-162.
17. Novoselov, K.S., et al., *Electric Field Effect in Atomically Thin Carbon Films.* Science, 2004. **306**(5696): p. 666-669.
18. Novoselov, K.S., et al., *Two-dimensional atomic crystals.* Proceedings of the National Academy of Sciences of the United States of America, 2005. **102**(30): p. 10451.
19. Gupta, A., T. Sakthivel, and S. Seal, *Recent development in 2D materials beyond graphene.* Progress in Materials Science, 2015. **73**: p. 44-126.

20. Nicolosi, V., et al., *Liquid Exfoliation of Layered Materials.* Science, 2013. **340**(6139).
21. Chhowalla, M., Z. Liu, and H. Zhang, *Two-dimensional transition metal dichalcogenide (TMD) nanosheets.* Chemical Society Reviews, 2015. **44**(9): p. 2584-2586.
22. Wang, Q.H., et al., *Electronics and optoelectronics of two-dimensional transition metal dichalcogenides.* Nat Nano, 2012. **7**(11): p. 699-712.
23. Wu, J.-Y., et al., *Photoluminescence of MoS_2 Prepared by Effective Grinding-Assisted Sonication Exfoliation*. Vol. 2014. 2014. 1-7.
24. Martincová, J., M. Otyepka, and P. Lazar, *Is Single Layer MoS_2 Stable in the Air?* Chemistry – A European Journal, 2017. **23**(53): p. 13233-13239.
25. Parzinger, E., et al., *Photocatalytic Stability of Single- and Few-Layer MoS_2.* ACS Nano, 2015. **9**(11): p. 11302-11309.
26. Ghatak, S., A.N. Pal, and A. Ghosh, *Nature of Electronic States in Atomically Thin MoS_2 Field-Effect Transistors.* ACS Nano, 2011. **5**(10): p. 7707-7712.
27. Lee, H.S., et al., *MoS_2 Nanosheet Phototransistors with Thickness-Modulated Optical Energy Gap.* Nano Letters, 2012. **12**(7): p. 3695-3700.
28. Li, X. and H. Zhu, *Two-dimensional MoS_2: Properties, preparation, and applications.* Journal of Materiomics, 2015. **1**(1): p. 33-44.
29. Radisavljevic, B., et al., *Single-layer MoS_2 transistors.* Nature Nanotechnology, 2011. **6**: p. 147.
30. Wang, Q.H., et al., *Electronics and optoelectronics of two-dimensional transition metal dichalcogenides.* Nature Nanotechnology, 2012. **7**: p. 699.
31. Fan, X.-L., et al., *Site-specific catalytic activity in exfoliated MoS_2 single-layer polytypes for hydrogen evolution: basal plane and edges.* Journal of Materials Chemistry A, 2014. **2**(48): p. 20545-20551.
32. Guardia, L., et al., *Chemically Exfoliated MoS_2 Nanosheets as an Efficient Catalyst for Reduction Reactions in the Aqueous Phase.* ACS Applied Materials & Interfaces, 2014. **6**(23): p. 21702-21710.
33. Lee, J.H., et al., *Efficient Hydrogen Evolution by Mechanically Strained MoS_2 Nanosheets.* Langmuir, 2014. **30**(32): p. 9866-9873.
34. Kalantar-zadeh, K. and J.Z. Ou, *Biosensors Based on Two-Dimensional MoS_2.* ACS Sensors, 2016. **1**(1): p. 5-16.
35. Bang, G.S., et al., *Effective Liquid-Phase Exfoliation and Sodium Ion Battery Application of MoS_2 Nanosheets.* ACS Applied Materials & Interfaces, 2014. **6**(10): p. 7084-7089.
36. Hwang, H., H. Kim, and J. Cho, *MoS_2 Nanoplates Consisting of Disordered Graphene-like Layers for High Rate Lithium Battery Anode Materials.* Nano Letters, 2011. **11**(11): p. 4826-4830.
37. Lu, S.-C. and J.-P. Leburton, *Electronic structures of defects and magnetic impurities in MoS_2 monolayers.* Nanoscale research letters, 2014. **9**(1): p. 676.
38. Song, I., C. Park, and H.C. Choi, *Synthesis and properties of molybdenum disulphide: from bulk to atomic layers.* RSC Advances, 2015. **5**(10): p. 7495-7514.
39. Splendiani, A., et al., *Emerging Photoluminescence in Monolayer MoS_2.* Nano Letters, 2010. **10**(4): p. 1271-1275.
40. Brent, J.R., N. Savjani, and P. O'Brien, *Synthetic approaches to two-dimensional transition metal dichalcogenide nanosheets.* Progress in Materials Science, 2017. **89**: p. 411-478.
41. Chhowalla, M., et al., *The chemistry of two-dimensional layered transition metal dichalcogenide nanosheets.* Nature Chemistry, 2013. **5**: p. 263.

42. Furchi, M.M., et al., *Mechanisms of Photoconductivity in Atomically Thin MoS_2.* Nano Letters, 2014. **14**(11): p. 6165-6170.
43. Liu, G.-B., et al., *Electronic structures and theoretical modelling of two-dimensional group-VIB transition metal dichalcogenides.* Chemical Society Reviews, 2015. **44**(9): p. 2643-2663.
44. Wang, L., et al., *Functionalized MoS_2 Nanosheet-Based Field-Effect Biosensor for Label-Free Sensitive Detection of Cancer Marker Proteins in Solution.* Small, 2014. **10**(6): p. 1101-1105.
45. Castellanos-Gomez, A., N. Agraït, and G. Rubio-Bollinger, *Optical identification of atomically thin dichalcogenide crystals.* Applied Physics Letters, 2010. **96**(21): p. 213116.
46. Dean, C.R., et al., *Boron nitride substrates for high-quality graphene electronics.* Nature Nanotechnology, 2010. **5**: p. 722.
47. Desai, S.B., et al., *Gold-Mediated Exfoliation of Ultralarge Optoelectronically-Perfect Monolayers.* Advanced Materials, 2016. **28**(21): p. 4053-4058.
48. Li, H., et al., *Fabrication of Single- and Multilayer MoS_2 Film-Based Field-Effect Transistors for Sensing NO at Room Temperature.* Small, 2011. **8**(1): p. 63-67.
49. Li, H., et al., *Preparation and Applications of Mechanically Exfoliated Single-Layer and Multilayer MoS_2 and WSe_2 Nanosheets.* Accounts of Chemical Research, 2014. **47**(4): p. 1067-1075.
50. Mak, K.F., et al., *Control of valley polarization in monolayer MoS_2 by optical helicity.* Nature Nanotechnology, 2012. **7**: p. 494.
51. Elías, A.L., et al., *Controlled Synthesis and Transfer of Large-Area WS_2 Sheets: From Single Layer to Few Layers.* ACS Nano, 2013. **7**(6): p. 5235-5242.
52. Laskar, M.R., et al., *Large area single crystal (0001) oriented MoS_2.* Applied Physics Letters, 2013. **102**(25): p. 252108.
53. Wu, S., et al., *Vapor–Solid Growth of High Optical Quality MoS_2 Monolayers with Near-Unity Valley Polarization.* ACS Nano, 2013. **7**(3): p. 2768-2772.
54. Zhou, W., et al., *Intrinsic Structural Defects in Monolayer Molybdenum Disulfide.* Nano Letters, 2013. **13**(6): p. 2615-2622.
55. Song, J.-G., et al., *Layer-controlled, wafer-scale, and conformal synthesis of tungsten disulfide nanosheets using atomic layer deposition.* ACS nano, 2013. **7**(12): p. 11333.
56. Zhang, Y., et al., *Controlled Growth of High-Quality Monolayer WS sub(2) Layers on Sapphire and Imaging Its Grain Boundary.* ACS Nano, 2013. **7**(10): p. 8963-8971-8963-8971.
57. Jung, Y., et al., *Metal Seed Layer Thickness-Induced Transition From Vertical to Horizontal Growth of MoS_2 and WS_2.* Nano Letters, 2014. **14**(12): p. 6842-6849.
58. Orofeo, C.M., et al., *Scalable synthesis of layer-controlled WS_2 and MoS_2 sheets by sulfurization of thin metal films.* Applied Physics Letters, 2014. **105**(8): p. 083112.
59. Park, J., et al., *Thickness modulated MoS_2 grown by chemical vapor deposition for transparent and flexible electronic devices.* Applied Physics Letters, 2015. **106**(1): p. 012104.
60. Zhan, Y., et al., *Large-Area Vapor-Phase Growth and Characterization of MoS_2 Atomic Layers on a SiO_2 Substrate.* Small, 2012. **8**(7): p. 966-971.
61. Tarasov, A., et al., *Highly Uniform Trilayer Molybdenum Disulfide for Wafer-Scale Device Fabrication.* Advanced Functional Materials, 2014. **24**(40): p. 6389-6400.
62. Wang, J., et al., *Direct growth of molybdenum disulfide on arbitrary insulating surfaces by chemical vapor deposition.* RSC Advances, 2015. **5**(6): p. 4364-4367.
63. Paton, K.R., et al., *Scalable production of large quantities of defect-free few-layer graphene by shear exfoliation in liquids.* Nature Materials, 2014. **13**: p. 624.

64. Varrla, E., et al., *Turbulence-assisted shear exfoliation of graphene using household detergent and a kitchen blender.* Nanoscale, 2014. **6**(20): p. 11810-11819.

65. Varrla, E., et al., *Large-Scale Production of Size-Controlled MoS_2 Nanosheets by Shear Exfoliation.* Chemistry of Materials, 2015. **27**(3): p. 1129-1139.

66. Coleman, J.N., et al., *Two-Dimensional Nanosheets Produced by Liquid Exfoliation of Layered Materials.* Science, 2011. **331**(6017): p. 568.

67. Cunningham, G., et al., *Solvent Exfoliation of Transition Metal Dichalcogenides: Dispersibility of Exfoliated Nanosheets Varies Only Weakly between Compounds.* ACS Nano, 2012. **6**(4): p. 3468-3480.

68. May, P., et al., *Role of Solubility Parameters in Understanding the Steric Stabilization of Exfoliated Two-Dimensional Nanosheets by Adsorbed Polymers.* The Journal of Physical Chemistry C, 2012. **116**(20): p. 11393-11400.

69. Smith, R.J., et al., *Large-Scale Exfoliation of Inorganic Layered Compounds in Aqueous Surfactant Solutions.* Advanced Materials, 2011. **23**(34): p. 3944-3948.

70. Yao, Y., et al., *Large-scale production of two-dimensional nanosheets.* Journal of Materials Chemistry, 2012. **22**(27): p. 13494-13499.

71. Notley, S.M., *Highly Concentrated Aqueous Suspensions of Graphene through Ultrasonic Exfoliation with Continuous Surfactant Addition.* Langmuir, 2012. **28**(40): p. 14110-14113.

72. Khan, U., et al., *High-Concentration Solvent Exfoliation of Graphene.* Small, 2010. **6**(7): p. 864-871.

73. Khan, U., et al., *Solvent-Exfoliated Graphene at Extremely High Concentration.* Langmuir, 2011. **27**(15): p. 9077-9082.

74. O'Neill, A., U. Khan, and J.N. Coleman, *Preparation of High Concentration Dispersions of Exfoliated MoS_2 with Increased Flake Size.* Chemistry of Materials, 2012. **24**(12): p. 2414-2421.

75. Savjani, N., et al., *MoS_2 nanosheet production by the direct exfoliation of molybdenite minerals from several type-localities.* RSC Advances, 2014. **4**(67): p. 35609-35613.

76. Kim, J., et al., *Direct exfoliation and dispersion of two-dimensional materials in pure water via temperature control.* Nature Communications, 2015. **6**: p. 8294.

77. Zhou, K.-G., et al., *A Mixed-Solvent Strategy for Efficient Exfoliation of Inorganic Graphene Analogues.* Angewandte Chemie International Edition, 2011. **50**(46): p. 10839-10842.

78. Ambrosi, A., Z. Sofer, and M. Pumera, *Lithium Intercalation Compound Dramatically Influences the Electrochemical Properties of Exfoliated MoS_2.* Small, 2014. **11**(5): p. 605-612.

79. Benavente, E., et al., *Intercalation chemistry of molybdenum disulfide.* Coordination Chemistry Reviews, 2002. **224**(1): p. 87-109.

80. Zeng, Z., et al., *Single-Layer Semiconducting Nanosheets: High-Yield Preparation and Device Fabrication.* Angewandte Chemie, 2011. **123**(47): p. 11289-11293.

81. Eda, G., et al., *Photoluminescence from Chemically Exfoliated MoS_2.* Nano Letters, 2011. **11**(12): p. 5111-5116.

82. Enyashin, A.N., et al., *New Route for Stabilization of 1T-WS_2 and MoS_2 Phases.* The Journal of Physical Chemistry C, 2011. **115**(50): p. 24586-24591.

83. Lukowski, M.A., et al., *Enhanced Hydrogen Evolution Catalysis from Chemically Exfoliated Metallic MoS_2 Nanosheets.* Journal of the American Chemical Society, 2013. **135**(28): p. 10274-10277.

84. Voiry, D., et al., *Conducting MoS_2 Nanosheets as Catalysts for Hydrogen Evolution Reaction.* Nano Letters, 2013. **13**(12): p. 6222-6227.

85. Posudievsky, O.Y., et al., *Improved dispersant-free liquid exfoliation down to the graphene-like state of solvent-free mechanochemically delaminated bulk MoS_2.* Journal of Materials Chemistry C, 2013. **1**(39): p. 6411-6415.

86. Yu, Y., et al., *Room temperature rubbing for few-layer two-dimensional thin flakes directly on flexible polymer substrates.* Scientific Reports, 2013. **3**: p. 2697.

87. Ren, X., et al., *One-step hydrothermal synthesis of monolayer MoS_2 quantum dots for highly efficient electrocatalytic hydrogen evolution.* Journal of Materials Chemistry A, 2015. **3**(20): p. 10693-10697.

88. Li, B.L., et al., *Electrochemically induced Fenton reaction of few-layer MoS_2 nanosheets: preparation of luminescent quantum dots via a transition of nanoporous morphology.* Nanoscale, 2014. **6**(16): p. 9831-9838.

89. Ibrahem, M.A., et al., *High quantity and quality few-layers transition metal disulfide nanosheets from wet-milling exfoliation.* RSC Advances, 2013. **3**(32): p. 13193-13202.

90. Johnson, D.W., B.P. Dobson, and K.S. Coleman, *A manufacturing perspective on graphene dispersions.* Current Opinion in Colloid & Interface Science, 2015. **20**(5): p. 367-382.

91. Parviz, D., et al., *Dispersions of non-covalently functionalized graphene with minimal stabilizer.* ACS nano, 2012. **6**(10): p. 8857-8867.

92. Friend, J. and L.Y. Yeo, *Microscale acoustofluidics: Microfluidics driven via acoustics and ultrasonics.* Reviews of Modern Physics, 2011. **83**(2): p. 647-704.

93. Ahmed, H., et al., *Ultrafast Acoustofluidic Exfoliation of Stratified Crystals.* Advanced Materials, 2018. **30**(20): p. 1704756.

94. Marqus, S., et al., *Increasing Exfoliation Yield in the Synthesis of MoS_2 Quantum Dots for Optoelectronic and Other Applications through a Continuous Multicycle Acoustomicrofluidic Approach.* ACS Applied Nano Materials, 2018. **1**(6): p. 2503-2508.

95. Destgeer, G. and H.J. Sung, *Recent advances in microfluidic actuation and micro-object manipulation via surface acoustic waves.* Lab on a Chip, 2015. **15**(13): p. 2722-2738.

96. Yeo, L.Y. and J.R. Friend, *Ultrafast microfluidics using surface acoustic waves.* Biomicrofluidics, 2009. **3**(1): p. 012002.

Chapter 3

3.1 Investigation of Layered MoS_2 Exfoliation by SAW in Solid Phase

In the first configuration used in our design, i.e., the production of QDs, the large particulates comprising the bulk MoS_2 feed in the enclosure were ejected from the substrate due to the tremendous surface acceleration $O(10^8\ m/s^2)$ that is generated on the substrate as the SAW traverses along it, subsequently colliding with the top and side walls of the enclosure (Figure 3.1(a,b)) and settling before being re-ejected. This ejection-collision-settling sequence occurs over many cycles. The ejection and collision events initially fragment aggregates present in the bulk powder feedstock into clumps that are approximately on the order of 100 μm in dimension, consistent with that observed in previous work in which the large substrate acceleration associated with the SAW was exploited for the deagglomeration of carbon nanotube bundles [1]. As shown in Figure 3.2 for two of the ejection--collision--settling cycles, it can be seen that over many cycles, however, the repetitive events lead to progressive fragmentation of the clumps beyond their deagglomeration, not just into individual flakes but also cleaving and thinning them down to monolayer and few-layer QDs. This is evident in the results shown in Figure 3.4, where increasing the exposure time of the SAW excitation—which is commensurate to increasing the number of ejection and collision cycles, and hence impact events—can be seen to lead to dimensional reduction of the MoS_2. After just 100 ms (or around 50 impact events, assuming

an in-flight velocity of 0.5 m/s, as estimated from the high-speed video images (Figure 3.3)), we were able to obtain fairly monodispersed 10 nm QDs of which around 90% consisted of either monolayers or two-layers (Figure 3.4(IV-d)).

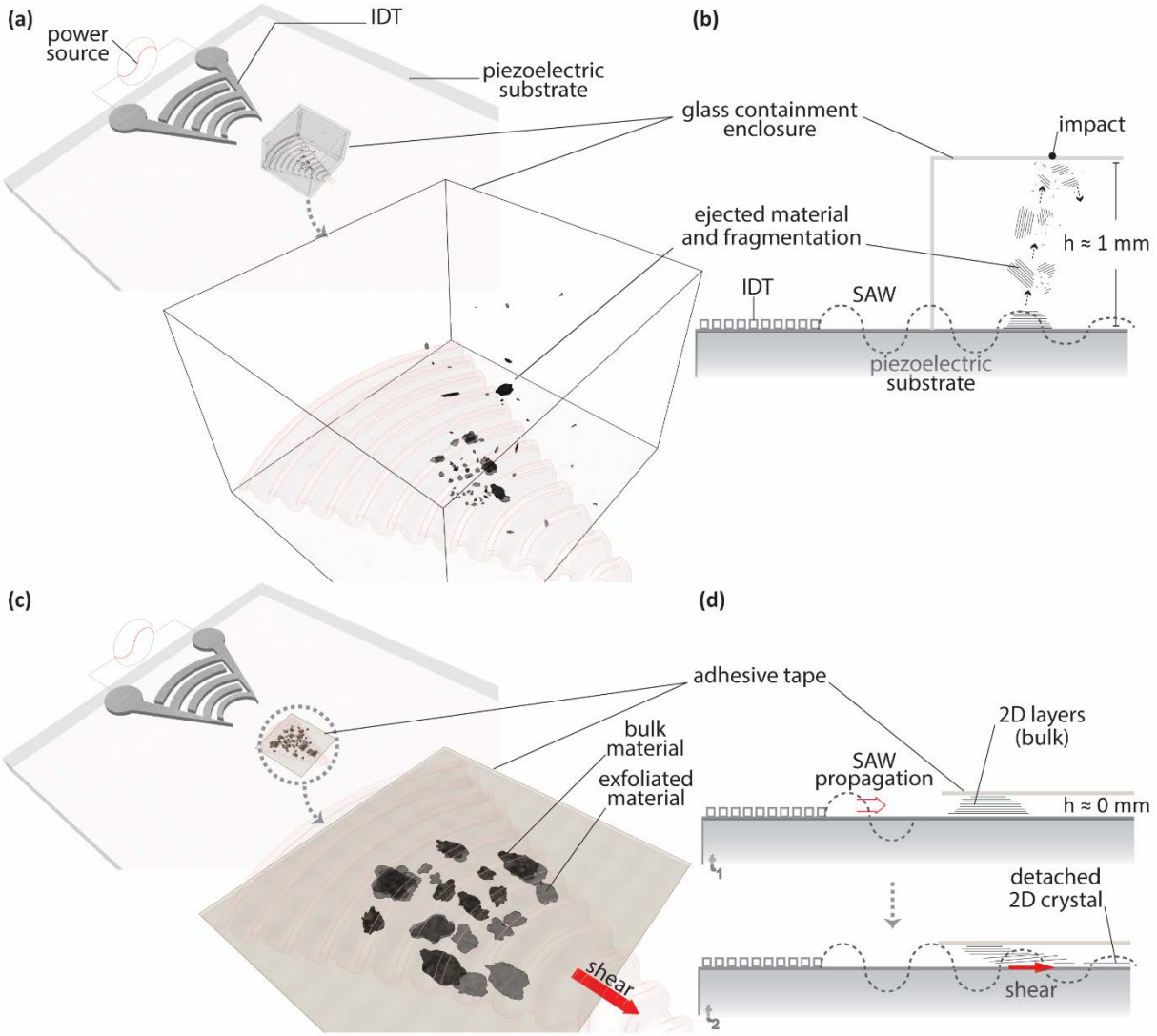

Figure 3.1. Schematic depiction of the device employed for dry exfoliation of MoS_2, in which two configurations of the experimental setup were explored. (a,b) Perspective and side view illustrations of the setup in which the bulk MoS_2 powder feedstock was contained within a glass enclosure and exfoliated into QDs via an impact mechanism involving multiple ejection-collision-settling cycles occurring within the enclosure due to the large SAW substrate acceleration. (c,d) Perspective and side view illustrations of the asymptotic zero-

height-limit setup in which the bulk MoS_2 powder feedstock was confined under adhesive tape such that it is progressively delaminated into large micron-sized sheets by the shear arising due to the SAW propagation along the substrate surface.

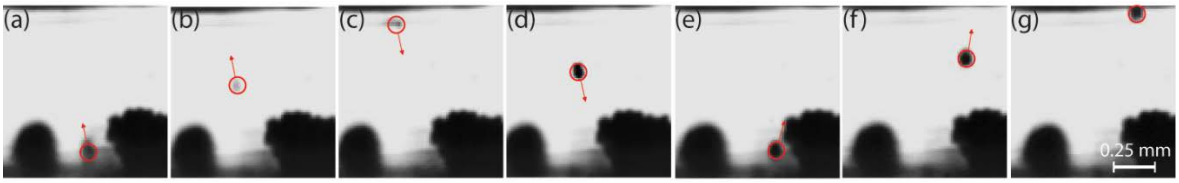

Figure 3.2. Sequence of images captured by high speed videography depicting the dominant mechanism for the exfoliation of bulk MoS_2 within the containment enclosure illustrated in Figure 3.1(a,b) for the production of QDs. (a-g) Two ejection--collision--settling cycle sequences over 6 ms in duration (1 ms increments between frames) wherein an MoS_2 powder cluster is progressively reduced in both height and lateral dimension upon impact with the walls of the enclosure.

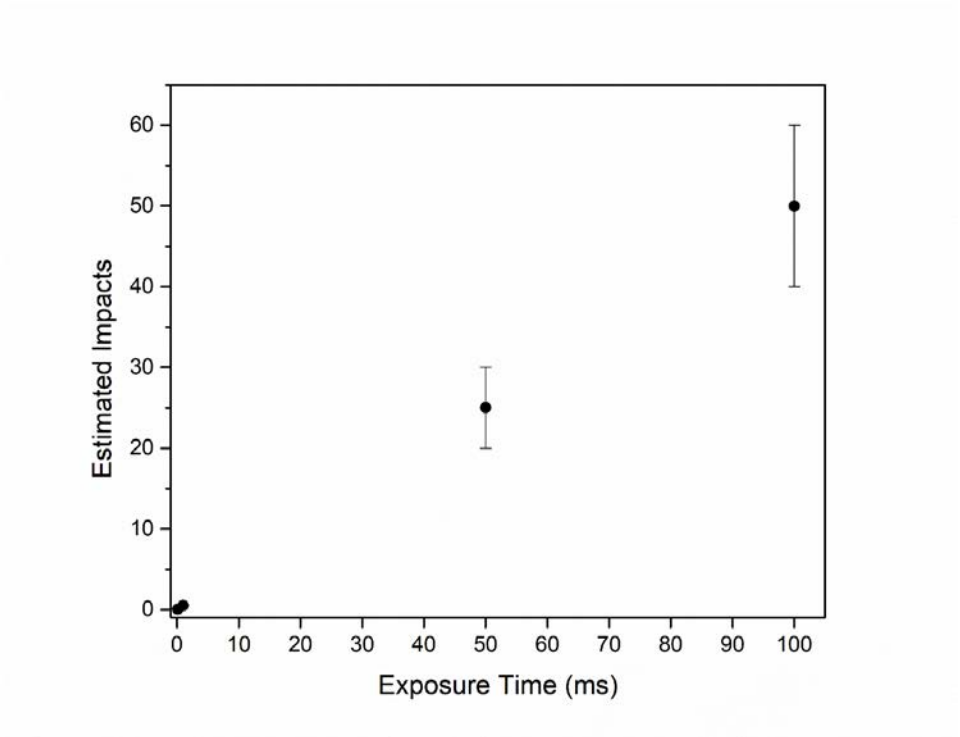

Figure 3.3. Typical particle cluster speeds upon impact, estimated from high speed videography, showing an average speed of 0.5 m/s.

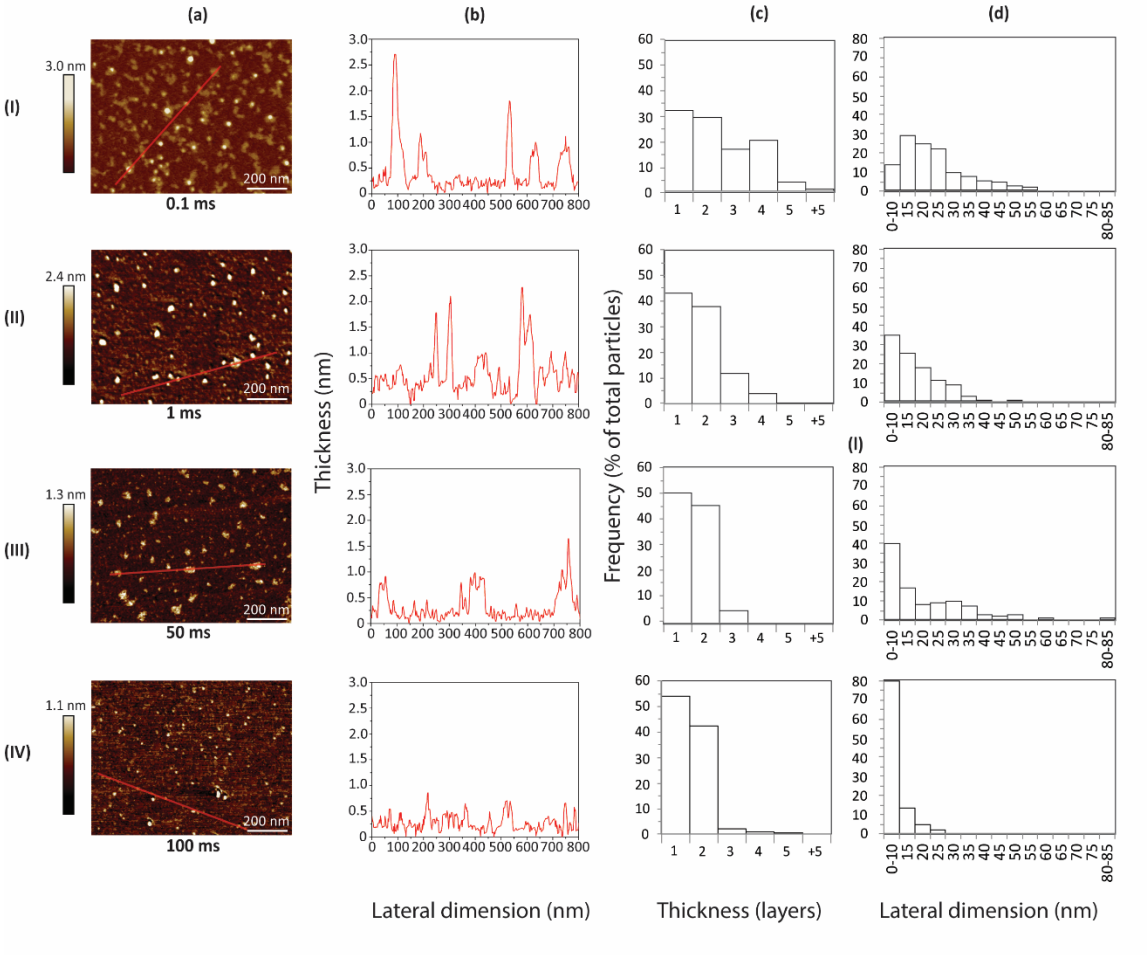

Figure 3.4. (a) AFM scans on mica sheet substrate and (b) height profiles, and, corresponding (c) thickness and (d) lateral dimension frequency distributions of the MoS_2 QDs, produced under impaction through multiple ejection--collision--settling cycles within the enclosure (Figure 3.1(a,b)) due to the large SAW substrate acceleration over different excitation times: (I) 0.1 ms, (II) 1 ms, (III) 50 ms, and, (IV) 100 ms.

Such impact-driven dimensional reduction is perhaps not surprising when the force experienced by a single MoS_2 flake during ejection is considered. For a substrate displacement amplitude ξ—estimated via laser Doppler vibrometry (UHF-120; Polytec Inc., Irvine, CA, USA) —of approximately 20 nm, we estimate a force $\rho L^2 h \omega^2 \xi$ of approximately 100 nN, which is on the order of that required for rupture of MoS_2 flakes induced by an AFM tip [2]; here ρ is the flake density, and, L and h are its lateral dimension and thickness,

respectively. Moreover, the AFM scans in Figure 3.4, as well as the PL intensity spectra in Figure 3.5 (see also Figure 3.6(a) where the data shows excitation at different wavelengths, exhibiting a progressive blue shift commensurate with a reduction in the dimensions of the material [3, 4] with increasing SAW exposure duration) suggest the possibility for flexibly tuning the QD synthesis, both in terms of their height (i.e., number of layers) and their lateral dimensions, simply through modulation of the incredibly short millisecond-order exposure time. AFM images were scanned after transfer to mica sheet substrate due to incompatibility of the piezoelectric nature of the substrate with the characterization technique, although $LiNbO_3$ substrate exhibits an ultra-smooth surface. Further characterization of the QDs with UV-Vis absorbance spectrometry can be found in the Figure 3.6(b) indicating a blue shift of the observed excitonic peaks in the absorption spectrum due to quantum size effect [5], as seen in AFM Figure 3.4 and HR-TEM Figure 3.8, and consistent with values reported in the literature [6-8]. Figure 3.6(a) also shows the overall collective PL behavior of the QDs, while powder XRD in Figure 3.7 indicates that the sample primarily comprises the 2H phase, HR-TEM in Figure 3.8 shows the sample size and crystallinity, and Figure 3.9 shows the quantum yield increase with increasing SAW exposure duration.

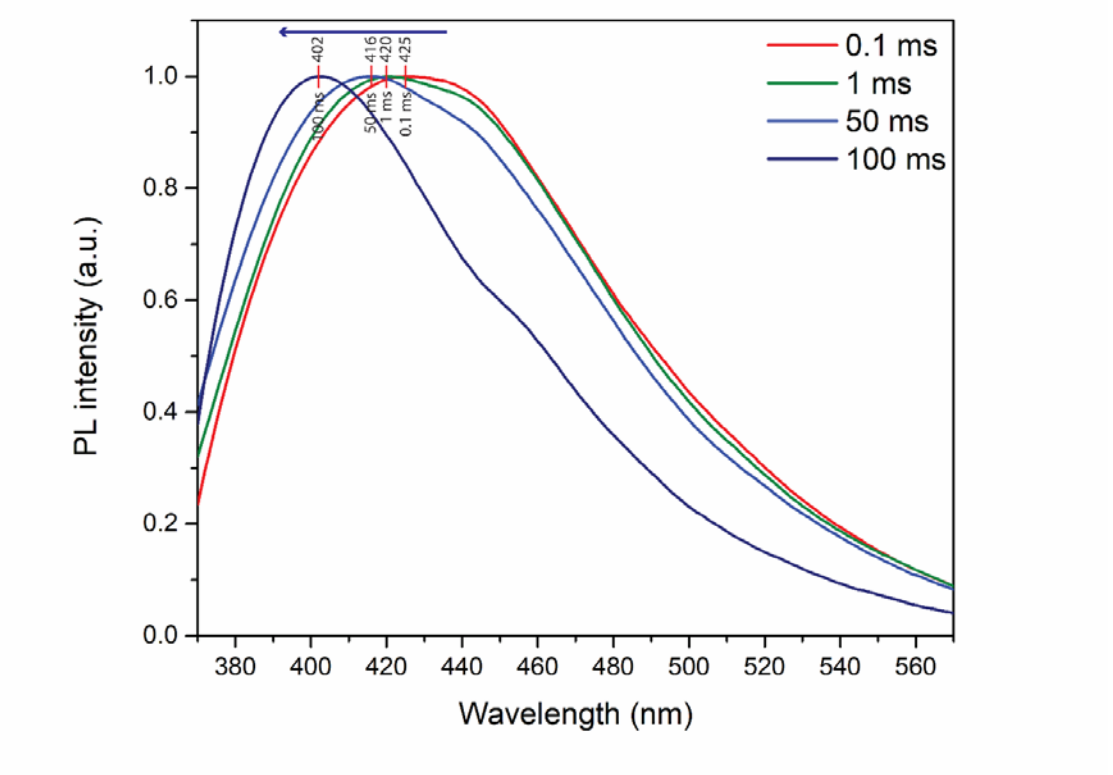

Figure 3.5. Normalized PL spectra of the QDs produced in the enclosure setup, depicted in Figure 3.1(a,b) for increasing SAW exposure times. A blueshift in the PL peak can be seen with increasing exposure duration.

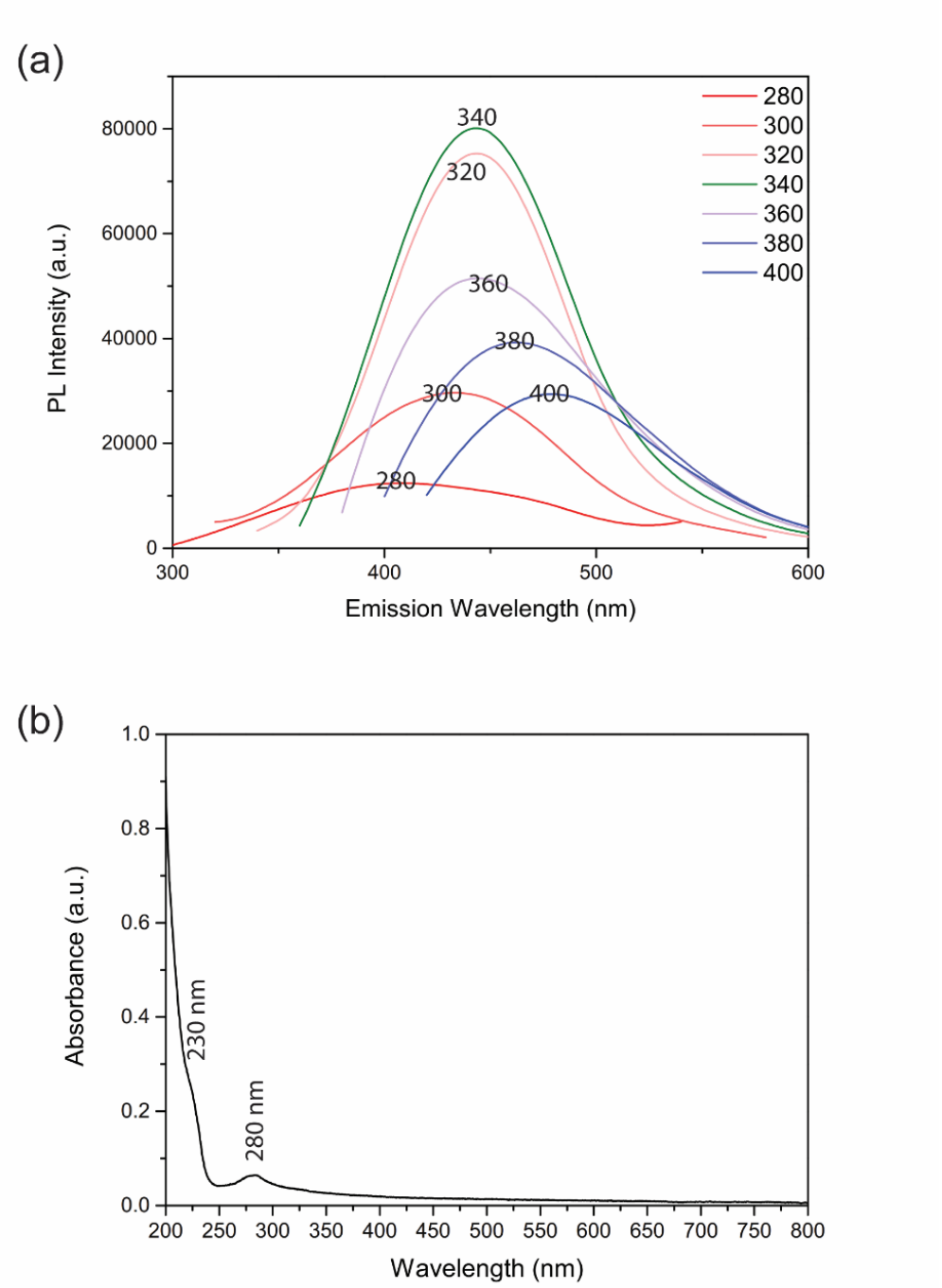

Figure 3.6. (a) PL spectrum of a dispersion of MoS_2 QDs irradiated at increasing wavelengths, in which a characteristic shift in the emission maxima is observed, thus indicating their polydisperse nature. (b) Absorbance spectrum of the MoS_2 QDs, showing characteristic peaks at 230 nm and 280 nm.

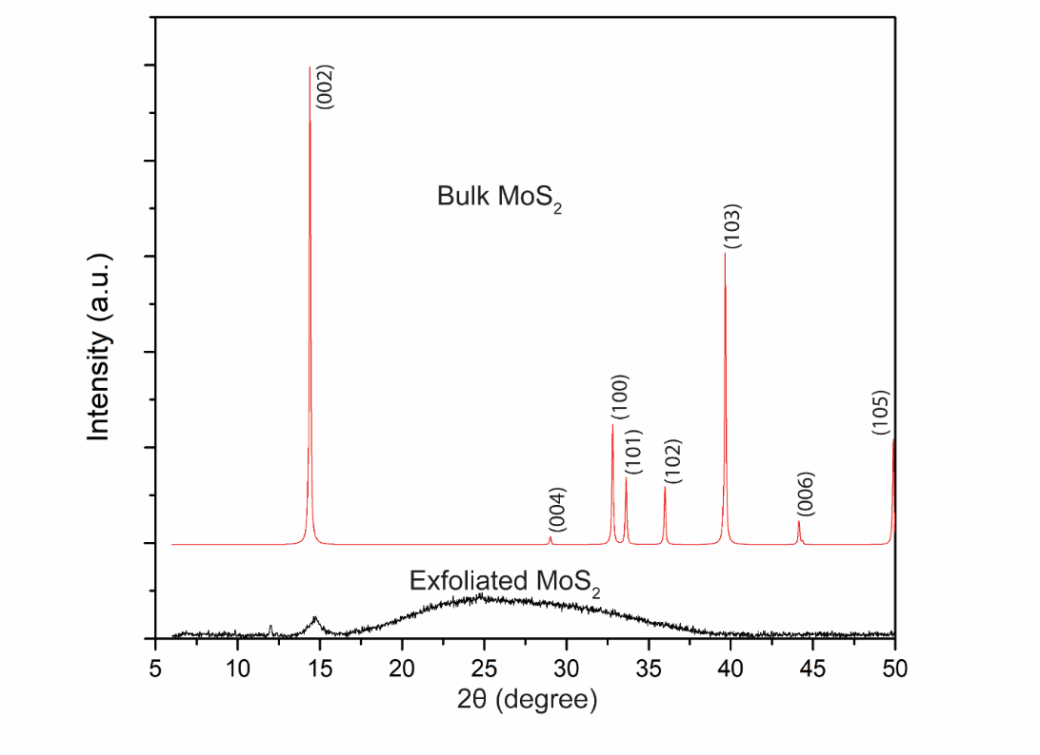

Figure 3.7. Powder XRD spectra of the exfoliated MoS_2 QDs in comparison to bulk MoS_2 on a glass substrate.

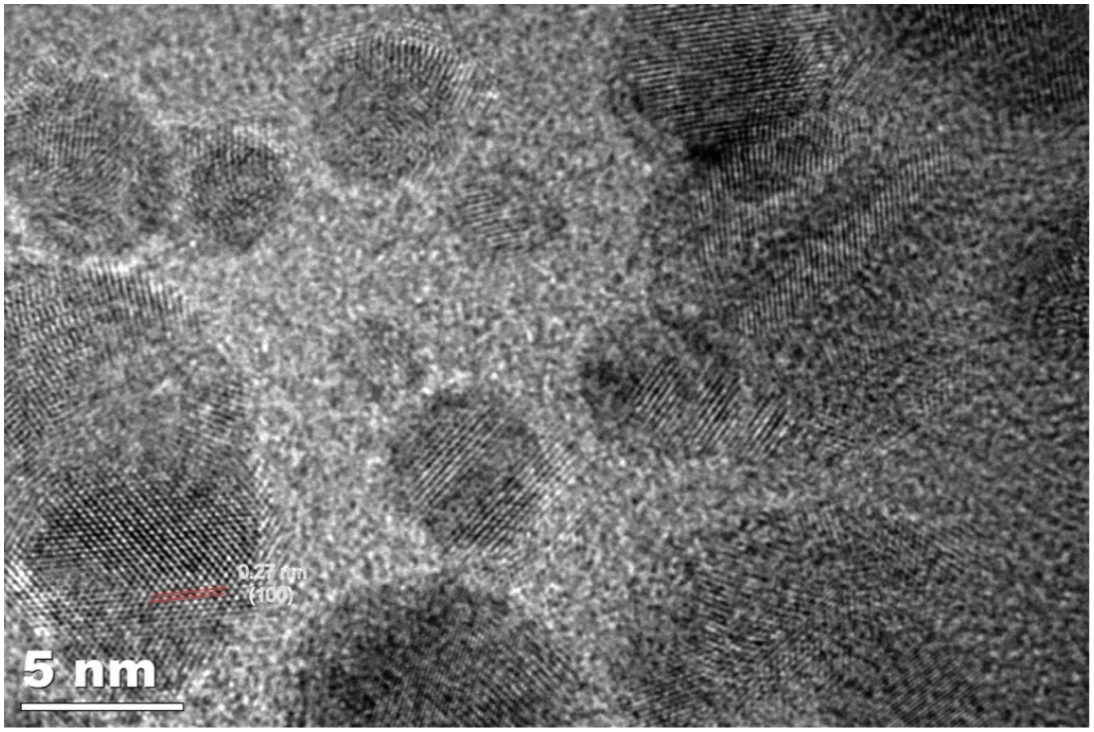

Figure 3.8. HR-TEM image of the MoS_2 QDs obtained, showing the 0.27 nm interlayer spacing corresponding to the (100) lattice plane.

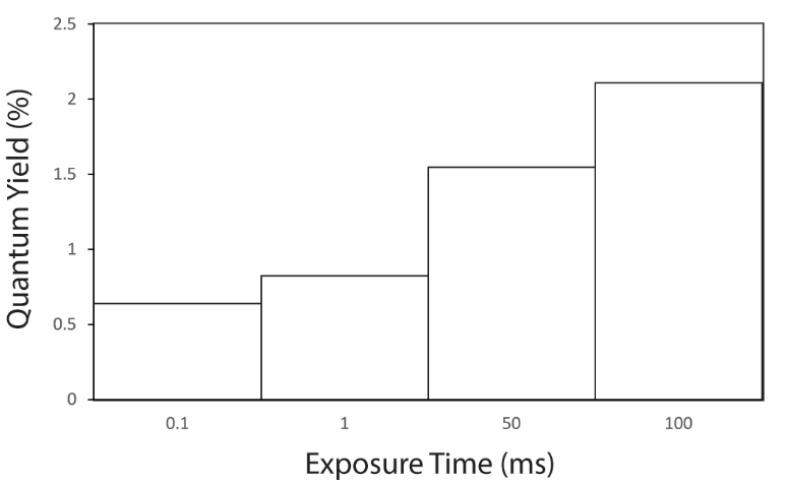

Fig. 3.9. Increasing quantum yield, as calculated from the spectrofluorometric data using quinine sulfate standard, with increase in the SAW exposure time.

The latter configuration, in which the bulk MoS_2 feed is confined beneath adhesive tape (Figure 3.1(c,d)), on the other hand, constitutes the asymptotic limit of zero-enclosure-height wherein all impact events (i.e., the ejection-collision-settling cycles) are suppressed. In this case, large MoS_2 sheets are produced in place of the QDs (Figure 3.10). This is because the impaction mechanism in the former enclosure configuration in Figure 3.1(a,b) primarily results in the reduction of the particulates in *both* dimensions, i.e., the thickness as well as the lateral dimension, on the other hand, suppressing the impact by confining the flakes to the substrate, in contrast, allows the shear force that arises as a consequence of the SAW propagation along the substrate surface to dominate such that the stacked layers in the material are progressively delaminated whilst preserving their lateral dimensions, regardless of the starting thickness of the bulk material. As seen by the resultant MoS_2 sheets in Figure 3.10(a,b) (see also the HR-TEM image of representative sheets in Figure 3.11 showing the crystalline nature of the sheets).

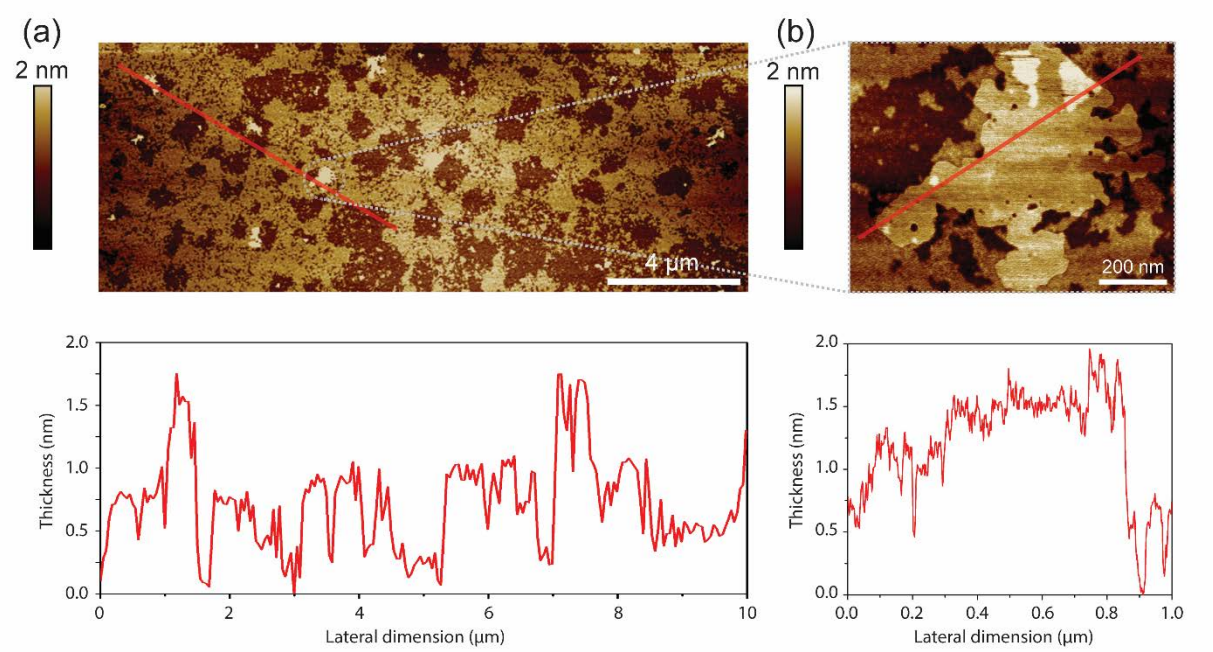

Figure 3.10. (a,b) AFM scans and height profiles of the large MoS_2 sheets, produced due to the shear as a consequence of the travelling SAW in the zero-height-limit enclosure case by confining the feed under adhesive tape, as depicted in Figure 3.1(c,d). The image and height profile in (b) is a magnification of one of the sheets found in (a).

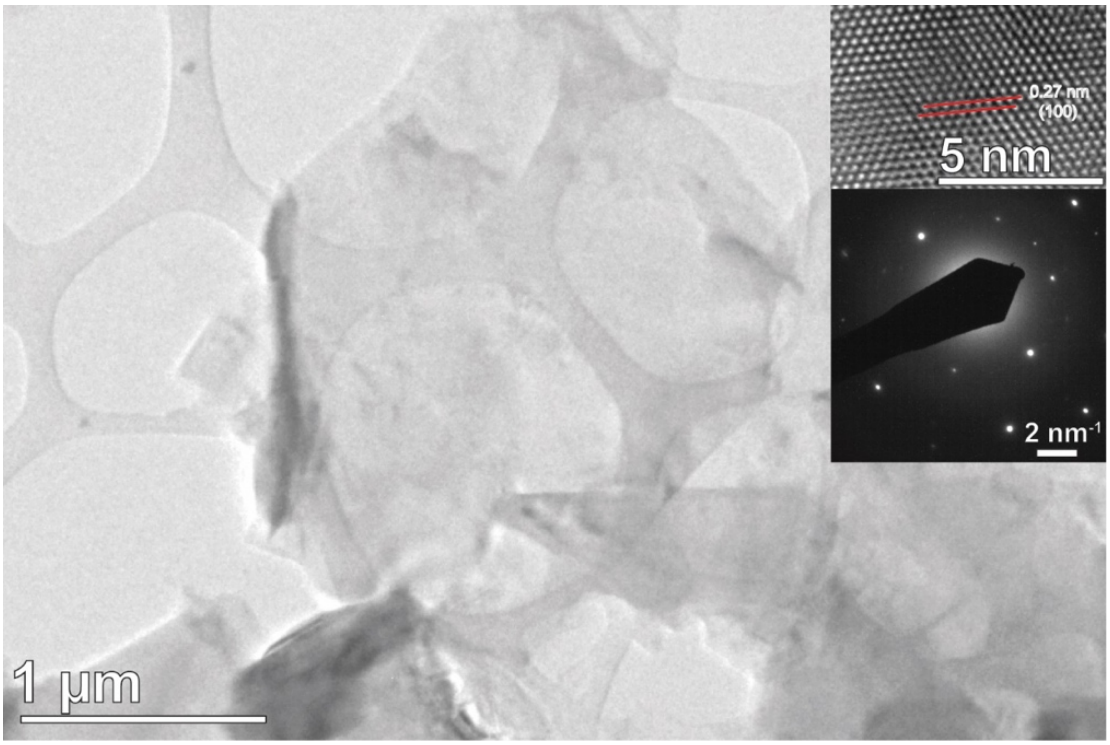

Fig. 3.11. HR-TEM image of the large MoS_2 sheets that are produced. The insets show the

characteristic interlayer spacing associated with the (100) plane and the corresponding diffraction pattern.

That travelling SAWs can give rise to sliding motion of a wide range of object sizes, be it for relatively large millimeter-scale objects such as sliders [9], micropropellers [10] or droplets [11-16],or small sub-micron objects such as nanowires [17] and even sub-atomic particles such as excitons [18], along the substrate surface has previously been reported. In each of these, including the present case, the SAW acts as a conveyor belt that translates these objects along its propagation direction. By immobilizing the topmost layer of the material to the adhesive tape in the present configuration (Figure 3.1(c,d)), the moving surface beneath successively shears individual layers of the material adjacent to it as the travelling SAW propagates, and subsequently transports them away from the parent cluster, as depicted in the schematic in Figure 3.1(d). As their lateral dimensions are more or less preserved due to the suppression of the impact force, we observe this technique to remarkably result in large, pristine monolayer sheets (Figure 3.10(a,b))---which is difficult to achieve with many other techniques [19].

Moreover, it can be seen that the sample is rich in sheets, thus allowing the production of a large (> 20 μm) coverage, most of which comprise single-layer sheets with the exception of a few that are made up of two layers. It should be noted that our characterization of the coverage is limited by the scan area of the AFM in order to preserve the tip sensitivity for single-layer measurements. As such, it may be possible that the monolayer coverage could be larger than the 20 μm that was observed. We further characterized the exfoliated sheets through powder XRD and Raman spectroscopy (Figures 3.12(a,b)) and show from the absorption spectra and corresponding excitonic peaks for four samples acquired for different SAW exposure durations and powers that the sheet concentration and yield can be tuned to some extent by increasing either the time or intensity

over which the samples are exposed to the SAW (Figure 3.12(c)), thus allowing the production rate of an already rapid exfoliation process to be increased.

(a)

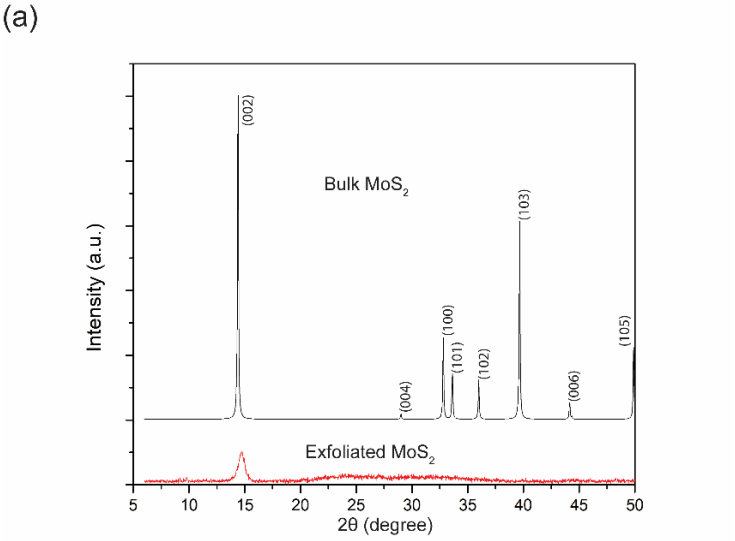

(b)

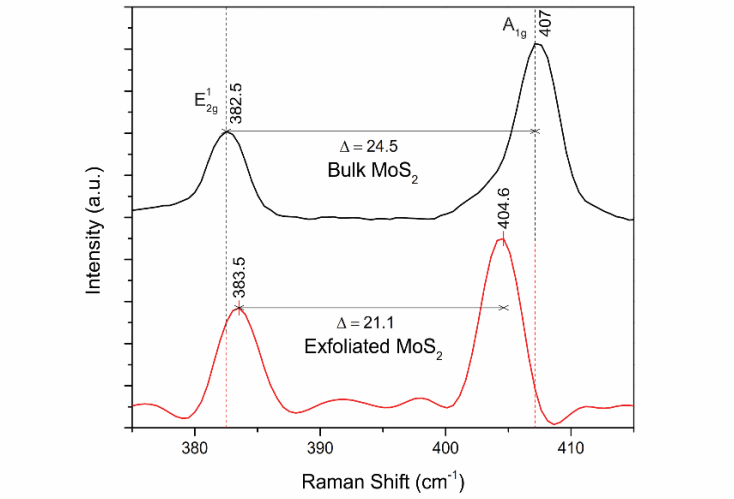

(c)

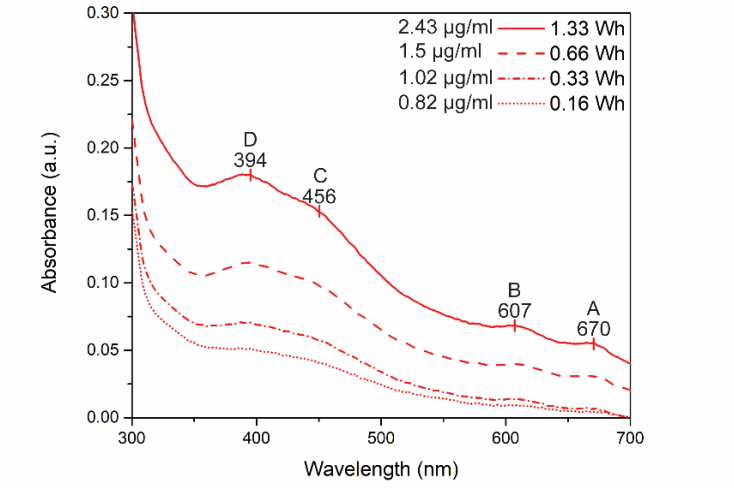

Figure 3.12. (a) Powder XRD and (b) Raman spectra of the exfoliated sheets in comparison to bulk MoS_2, and, (c) UV/Vis absorbance spectra of the former at different SAW energies together with the corresponding exfoliated product concentration. A, B, C and D are the excitonic peaks, which can be seen to increase in intensity with increasing SAW exposure. The samples represent from bottom to up: 1 minute exposure at two different powers, and 5 minutes exposure at the same two power settings.

The longer exposure time is explained by the set lower power input for MoS_2 sheets production relative to that used for quantum dots. The aim is to carefully suppress impacts to preserve the lateral dimensions.

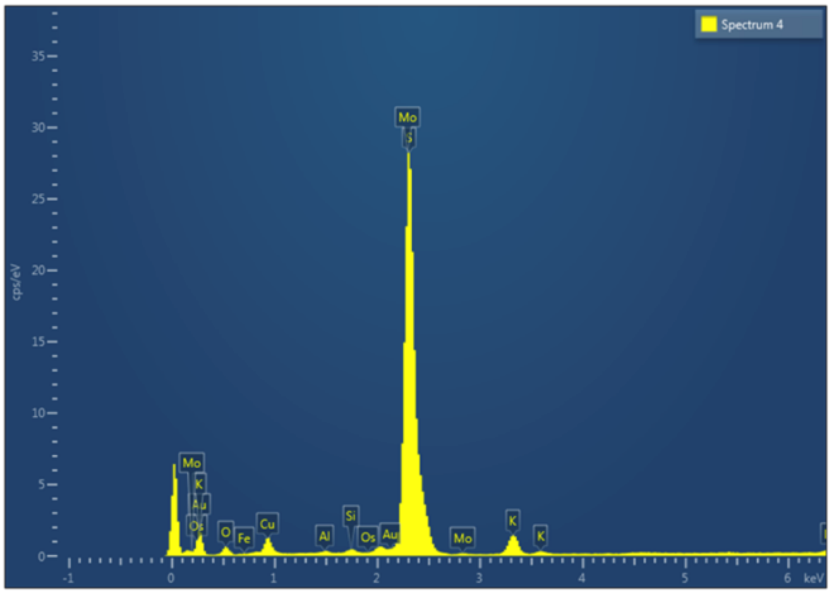

Element	Atomic %
C	76.9
O	12.6
S	6.8
Mo	3.2
K	0.1
Si	0.2
Cu	0.2
Ti	0
Fe	0

Figure 3.13. TEM-EDS elemental analysis of the produced MoS_2 sheets, nearly 1 Mo : 2 S atoms ratio can be seen in the attached table. Other elements are attributed to the underlying TEM carbon grid.

Although some defects could occur as with any high shear-based exfoliation method, the most common defect is the release of one of the attached sulfur atoms [20]. The EDX performed on the MoS_2 flakes produced, however, reveals a stochiometric ratio of nearly 1 Mo : 2 S atoms, indicating preservation of the sample with no oxidation. The result indeed

confirms the elemental analysis by X-ray photoelectron spectroscopy (XPS) on MoS_2 after SAW exposure, where application of SAW on MoS_2 for the purpose of photoluminescence manipulation [21] was shown not to alter the chemical nature of the material. Another technique that can detect MoS_2 defects is Raman spectroscopy at a much lower frequency range (150-330 cm^{-1}) than the one characteristic to MoS_2 interlayers interaction and sheet thickness [20].

Furthermore, the proposed platform can be considered as a highly non-invasive exfoliation technique as it is does not introduce chemical or physical agents that may affect the quality of the end product; due to the fact that it is both solvent and additive-free, in addition to not altering MoS_2 chemical nature with the direct application of SAW [21]. The minimal residual heat generated by SAW device does not affect the stability of MoS_2, as the operation temperature (< 50 °C) never exceeded the limit for its oxidation [22] within the power range applied for either QDs or sheets production. The heat was further completely dissipated by employing pulsation of RF signal generating SAW allowing time for the chip to cool to ambient temperature in the off period. Another reason for the pulse mode operation is preservation of the substrate structural integrity from repeated SAW exposures. Therefore, remarkable qualities of pristine exfoliated MoS_2 are preserved, while not compromising tunability or scalability through massive parallelization of the miniaturized platform. Other materials exfoliation in the platform depends highly on van der Waals forces strength holding the stack of 2D layers, for thinning, and the tensile strength, for lateral size reduction. Therefore, it is estimated that relatively more power would be required to be applied and in turn more intense SAW for materials with larger stiffness to reach its breaking point [23]. In addition, enhancing the applied electric field coupled with a piezoelectric nature of the material can highly synergize the process [24].

3.2 Materials and Methods

The schematics in Figure 3.1 provide an illustration of the experimental setup, comprising the single-crystal piezoelectric lithium niobate (128° *Y*-rotated, *X*-propagating $LiNbO_3$; Roditi Ltd., London, UK) chip-scale substrate on which the SAW propagates. The SAW itself is generated by applying an oscillating electrical signal at resonance from a signal generator (SML01; Rhode & Schwarz, North Ryde, NSW, Australia) and amplifier (LYZ-22+; Mini Circuits, Brooklyn, NY, USA) to focused interdigitated transducer electrodes (IDTs) consisting of sixty 5-mm-wide interleaved finger pairs with a gap and spacing that corresponds to one-eighth of the SAW wavelength λ = 132 µm and hence its resonant frequency ω = 30 MHz. The IDTs, which comprise single-phase unidirectional transducer (SPUDT) designs, wherein acoustic reflectors are inserted between the electrode fingers such that the SAW only propagates in the forward direction (i.e., the waves constructively interfere in the forward direction and destructively in the reverse), were patterned onto the chip by sputter coating (SPI-Module Sputter Coater; Structure Probe Inc., West Chester, PA, USA) a 10 nm chromium adhesion layer followed by a 500 nm aluminium layer onto the substrate, followed by etching using standard photolithography techniques.

Depending on whether the nanoscale QDs or large micron sheets are desired, we either contained 5 mg of bulk MoS_2 powder (6 µm, 99.9% purity (US1089M, CAS: 1317-33-5); US Research Nanomaterials Inc., Houston, TX, USA) within a custom-made glass enclosure of dimensions 5 mm × 5 mm × 1 mm (Figure 3.1(a,b)), or confined 1 mg of bulk MoS_2 powder under thermal adhesive tape (Graphene Square, Fort Lee, NJ, USA) and a 1 g load (Figure 3.1(c,d)) prior to their excitation with the SAW. In the former, the input power was 1 mW prior to amplification with a 20% duty cycle (50 ms per 250 ms), whereas we employed either 0.05 mW or 0.2 mW subject to a 50% duty cycle (50 ms per 100 ms) in the latter; regular tape was also used in place of the thermal adhesive with no effect on the result, although this

required an additional wash step with 45% ethanol after the exfoliation. To release the exfoliated particles from the tape in the latter case, we heat the device to 100 °C for 3 mins as recommended by the manufacturer. The particulate product comprising the exfoliated MoS_2 from either case was collected in a microcentrifuge tube (Eppendorf South Pacific Pty.~Ltd., North Ryde, NSW, Australia) and suspended in 1 ml 45% ethanol in deionized water (18.2 MΩ.cm, Milli-Q; Merck Millipore, Bayswater, VIC, Australia), prior to being centrifuged (10,000 rpm for 20 mins in the former case and 2,000 rpm for 5 mins in the latter case) to separate the supernatant containing the exfoliated product from the remaining bulk material. We note that this final step involving collection in a solvent was only required for size fractionation for characterization of the sample; collection of the exfoliated product powder in dry stable form is possible since they are not bound to the substrate.

The MoS_2 QDs or sheets that were collected were then deposited onto a mica substrate and dried overnight in vacuum at room temperature prior to Atomic Force Microscopy (AFM) imaging (Multimode 8 with PeakForce Tunneling (TUNA) module; Bruker Corp., Santa Barbara, CA, USA). For high resolution Transmission Electron Microscopy (HR-TEM; Tecnai F20, FEI, Hillsboro, OR, USA), the samples were instead dried at room temperature on a carbon grid, on which they were imaged under an accelerating voltage of 200 kV. AFM images were flattened at 0.5 nm *z*-threshold and the analyses to measure their thicknesses and lateral dimensions were carried out using the supplied software (NanoScope, v1.8; Bruker Corp., Santa Barbara, CA, USA). We analyzed at least 100 particles per experimental condition. Powder x-ray diffraction (XRD) of exfoliated MoS_2 (D8 Advance, Bruker Pty. Ltd., Preston, VIC, Australia) with Cu K α radiation at 40 mA and 40 kV (λ = 1.54 Å) at a scan rate of $2°.min^{-1}$, step size of 0.02° and a 2Θ range of 6° to 90° on a glass substrate was compared to bulk powder data (Crystallography Open Database [25, 26] information card entry 1010993 [27]). Raman spectroscopy of the exfoliated product was, on the other hand,

carried out via excitation at 532 nm (10 mW, 370-420 cm^{-1} acquisition range, LabRAM HR Evolution; Horiba Ltd., Kyoto, Japan) whereas UV/Vis absorbance, photoluminescence (PL) and fluorescence measurements were performed using a quartz cuvette (10 mm path length, FireFlySci 701MFL; Quark Photonics Pty.~Ltd., Melbourne, VIC, AU) in a UV/Vis spectrophotometer (Cary 50 UV-Vis; Varian Inc., Santa Clara, CA, USA) and UV/Vis spectrofluorometer (Fluoromax-4P; Horiba Ltd., Kyoto, Japan). The Quantum yield of MoS_2 QDs was determined in relation to quinine sulfate standard in 0.1 M H_2SO_4 with known yield of 0.546 [28, 29], and calculated as stated in the references therein.

3.3 References

1. Miansari, M., et al., *Vibration-Induced Deagglomeration and Shear-Induced Alignment of Carbon Nanotubes in Air.* Advanced Functional Materials, 2014. **25**(7): p. 1014-1023.
2. Bertolazzi, S., J. Brivio, and A. Kis, *Stretching and Breaking of Ultrathin MoS_2.* ACS Nano, 2011. **5**(12): p. 9703-9709.
3. Gan, Z.X., et al., *Quantum confinement effects across two-dimensional planes in MoS_2 quantum dots.* Applied Physics Letters, 2015. **106**(23): p. 233113.
4. Lin, H., et al., *Colloidal synthesis of MoS_2 quantum dots: size-dependent tunable photoluminescence and bioimaging.* New Journal of Chemistry, 2015. **39**(11): p. 8492-8497.
5. Chikan, V. and D.F. Kelley, *Size-Dependent Spectroscopy of MoS_2 Nanoclusters.* The Journal of Physical Chemistry B, 2002. **106**(15): p. 3794-3804.
6. Fahimi-Kashani, N., et al., *MoS_2 quantum-dots as a label-free fluorescent nanoprobe for the highly selective detection of methyl parathion pesticide.* Analytical Methods, 2017. **9**(4): p. 716-723.
7. Wang, Y. and Y. Ni, *Molybdenum Disulfide Quantum Dots as a Photoluminescence Sensing Platform for 2,4,6-Trinitrophenol Detection.* Analytical Chemistry, 2014. **86**(15): p. 7463-7470.
8. Xing, W., et al., *MoS_2 Quantum Dots with a Tunable Work Function for High-Performance Organic Solar Cells.* ACS Applied Materials & Interfaces, 2016. **8**(40): p. 26916-26923.
9. Sakano, K., M.K. Kurosawa, and T. Shigematsu, *Driving Characteristics of a Surface Acoustic Wave Motor using a Flat-Plane Slider.* Advanced Robotics, 2010. **24**(10): p. 1407-1421.
10. Shilton, R.J., et al., *Rotational microfluidic motor for on-chip microcentrifugation.* Applied Physics Letters, 2011. **98**(25): p. 254103.
11. Wixforth, A., et al., *Acoustic manipulation of small droplets.* Analytical and bioanalytical chemistry, 2004. **379**(7-8): p. 982-991.
12. Tan, M.K., J.R. Friend, and L.Y. Yeo, *Direct visualization of surface acoustic waves along substrates using smoke particles.* Applied Physics Letters, 2007. **91**(22): p. 224101.
13. Renaudin, A., et al., *Creeping, walking and jumping drop.* Physics of Fluids, 2007. **19**(9): p. 091111.
14. Brunet, P., et al., *Droplet displacements and oscillations induced by ultrasonic surface*

acoustic waves: A quantitative study. Physical Review E, 2010. **81**(3): p. 036315.
15. Baudoin, M., et al., *Low power sessile droplets actuation via modulated surface acoustic waves.* Applied Physics Letters, 2012. **100**(15): p. 154102.
16. Bussonnière, A., et al., *Dynamics of sessile and pendant drops excited by surface acoustic waves: Gravity effects and correlation between oscillatory and translational motions.* Physical Review E, 2016. **93**(5): p. 053106.
17. Chen, Y., et al., *Tunable Nanowire Patterning Using Standing Surface Acoustic Waves.* ACS Nano, 2013. **7**(4): p. 3306-3314.
18. Rezk, A.R., et al., *Acoustically-Driven Trion and Exciton Modulation in Piezoelectric Two-Dimensional MoS_2.* Nano Letters, 2016. **16**(2): p. 849-855.
19. Brent, J.R., N. Savjani, and P. O'Brien, *Synthetic approaches to two-dimensional transition metal dichalcogenide nanosheets.* Progress in Materials Science, 2017. **89**: p. 411-478.
20. Lin, Z., et al., *Defect engineering of two-dimensional transition metal dichalcogenides.* 2D Materials, 2016. **3**(2): p. 022002.
21. Rezk, A.R., et al., *Acoustic–Excitonic Coupling for Dynamic Photoluminescence Manipulation of Quasi-2D MoS_2 Nanoflakes.* Advanced Optical Materials, 2015. **3**(7): p. 888-894.
22. Martincová, J., M. Otyepka, and P. Lazar, *Is Single Layer MoS_2 Stable in the Air?* Chemistry – A European Journal, 2017. **23**(53): p. 13233-13239.
23. Jiang, J.-W., *Graphene versus MoS_2: A short review.* Frontiers of Physics, 2015. **10**(3): p. 287-302.
24. Ahmed, H., et al., *Ultrafast Acoustofluidic Exfoliation of Stratified Crystals.* Advanced Materials, 2018. **30**(20): p. 1704756.
25. Grazulis, S., et al., *Crystallography Open Database - an open-access collection of crystal structures.* Journal of Applied Crystallography, 2009. **42**(4): p. 726-729.
26. Gražulis, S., et al., *Crystallography Open Database (COD): an open-access collection of crystal structures and platform for world-wide collaboration.* Nucleic Acids Research, 2012. **40**(D1): p. D420-D427.
27. Dickinson, R.G. and L. Pauling, *THE CRYSTAL STRUCTURE OF MOLYBDENITE.* Journal of the American Chemical Society, 1923. **45**(6): p. 1466-1471.
28. Melhuish, W., *Quantum efficiencies of fluorescence of organic substances: effect of solvent and concentration of the fluorescent solute1.* The Journal of Physical Chemistry, 1961. **65**(2): p. 229-235.
29. Eaton, D.F., *Reference materials for fluorescence measurement.* Pure and Applied Chemistry, 1988. **60**(7): p. 1107-1114.

Chapter 4

Conclusions & Future Directions

In this chapter, a brief overview of the work carried out in this thesis is presented, highlighting the significance of the contribution made to the current body of knowledge in the field of study. Then, prospective applications are suggested building on this work.

Throughout the thesis, we have demonstrated a novel miniature platform on a chip-scale for rapid solvent- and additive-free exfoliation of MoS_2 to either small nanometer scale QDs or large micron dimension sheets. The former exfoliated product is produced through an impaction mechanism of ejection–collision–settling cycles made possible by a miniature enclosure design, which holds the bulk material feed in powder form on a $LiNbO_3$ piezoelectric substrate, and a tremendous piezoelectric surface acceleration of 10^8 m/s^2 in nano-displacement component perpendicular to the surface on which the travelling SAW propagates. The latter exfoliated product is made in a zero-height limit enclosure by confinement of the bulk material feed under adhesive tape to ensure that the bulk material particles are always directly in contact with the piezoelectric substrate and to suppress the aforementioned ejection–collision–settling cycles; therefore, the shearing component of the travelling SAW parallel to the surface becomes the prominent acting force instead of the impaction force with the surface, thus, allowing the lowermost layers of the bulk stack held by the adhesive tape to progressively delaminate in a manner similar to a conveyer belt.

Further, we showed the tuneability of the platform for either of the 0D nanometer-sized

QDs or the 2D micron-sized sheets of MoS_2 material. The QDs can be tuned in lateral dimension as well as thickness down to monolayers by controlling the exposure time to SAW or its power, which affects the frequency of impacts and their force affecting both the delamination towards monolayers and cleavage to QDs in nano-size domain. On the other hand, the sheets production can be tuned to some extent regarding the product yield by controlling the energy input to the exfoliation process, i.e. time of exposure to SAW and power used to produce SAW, due to the design that limits the action of SAW to delamination from bulk 2D material and minimizes the lateral size reduction.

The extreme acceleration on the piezoelectric surface by SAW greatly increases the force of impact; therefore, the required exposure time to observe a significant exfoliation in bulk 2D materials / particle size reduction and concurrent de-aggregation of powder is greatly reduced to ultrafast milliseconds exposure. In the asymptotic zero-height-limit setup for sheets production, the exfoliation process was rapid producing a significant yield in only minutes, albeit being relatively less than the miniature enclosure setup. The suppression of the impact and ejection cycles by design limited the role of time to increasing the delivered energy for the exfoliation process only and consequently the sheets yield. Another aspect was the applied power for the exfoliation process, which followed the same positive trend as that observed with increased exposure time. In addition, we note that the power applied to generate SAW on the miniature chip was manageable and suitable for either a portable design or massive parallelization route.

In this thesis, during the review of the various current techniques employed to synthesize 2D materials by either achieving exfoliation of bulk 2D material in the different top-down approaches, or building the 2D material single crystal in bottom-up approach, we have shown the limitations of each technique that made no one method take a favored position as the approach of choice with maximum compatibility for the different subsequent

applications, despite the advantages each offered. The strong dependence of the 2D material characteristics on the quality, and hence use in a particular application, made any trade-off to the quality of the final product a major drawback. Even when pristine quality was attained in few of the techniques reviewed, there was a compromise in the yield or ability for scaling-up production. In comparison to CVD and other bottom-up approaches, the presented platform presents a cost effective, ultra-fast, tunable and scalable alternative. In addition, the platform does not require complexity, extreme conditions and skill generally needed to operate bottom-up approach processes, especially the transfer of the product to the final desired substrate as the crystal is bound to a primary substrate during synthesis. Regarding top-down chemical exfoliation methods and softer less invasive liquid exfoliation methods as the sonic assisted solvent exfoliation, Our platform offers a large advantage over these methods, which is the conservation of quality in solvent- and additive free technique added to the finer control over thickness and lateral dimension of the exfoliated layered 2D material. Although chemical exfoliation excels over any other technique in yield due to the harsh conditions employed, the process affects not only the size of the product, but it alters the crystal phase. The use of ultrasonication assisted liquid exfoliation, with either a good solvent of a suitable surface energy or a surfactant additive that modifies the solvent surface energy, brings the problems of product quality and additive or solvent residue, even after extensive post processing, as well as hard to attain tuneability, despite the advantage of scalability in liquid exfoliation techniques. Finally, the review of mechanical exfoliation techniques has shown that major progress has been made since the original simple adhesive tape technique was used. The very low yield, time-consuming, multistep process and extremely skill-dependent process was a compromise to having pristine micron-dimension largely monolayer sheets that were produced in a similar dry solvent- and additive-free condition to our platform. However, the technique was unable to produce QDs, lacked tuneability, had little run-to-run reproducibility of the flake dimensions

and thicknesses and most importantly had little potential for scalability. Later developments enhanced the technique by introducing scalability as in ball milling with a surfactant powder for later suspension in a liquid or alternatively the use of grinding with a water-soluble abrasive. These approaches had the side effect of large processing time to attain a significant yield and little control over the size reduction process. Moreover, the introduction of an additive even in a dry form necessitated an additional processing step for its removal that is not always efficient and was bound to keep traces of the additive affecting the 2D material product quality. In comparison to our proposed platform's powder product that does not employ any additives and the purity of the material is maintained throughout the whole exfoliation process, the exfoliated dry milled powder required an additional step before the size fractionation to obtain the usable exfoliated portion of the 2D material. Such extra processing step, even when the process is designed to use only deionized water solvent, further hindered the ready use of such techniques' exfoliated powder product as a stock. Other developments in mechanical exfoliation rather maintained the peeling action approach, facilitated relatively higher yield synthesis of sheets that are several hundreds of microns in dimension and integrated their transfer onto a specific substrate desired for a particular application, albeit at the expense of introducing more complexity, requiring additives that comprised more aggressive etchants additive and the lack of tunability or scalability.

We have demonstrated the SAW assisted dry exfoliation platform advantage over the current techniques in ultra-speed operation, tuneability and scalability of the miniature chip-scale platform, but most importantly the preservation of the 2D material quality through the lack of any solvents or additives and employment of purely mechanical process by acoustic radiation for exfoliation. The chemical nature of the 2D material is preserved as well, because the SAW does not alter the material in the experimental conditions employed proving the platform to be a highly non-invasive exfoliation technique. Furthermore, the

simplicity and low-cost of the process facilitates production intensification towards larger-scale yields through massive parallelization of the miniaturized chip-scale setup.

Other than the promising potential for lab scale or even industrial scale production through massive parallelization of the miniature chip that has low-cost, ultra-fast operation and low power demand. A move in the opposite direction towards portability makes the platform well suited towards powder de-aggregation of non-layered materials when incorporated in dry powder inhalation devices, which could enhance the efficacy of the drug delivered, minimize the use of additives in formulation, and further reduces the cost in a reusable platform.

A major advantage of the proposed platform stems from the versatility of its 2D material production from QDs with tunable thickness and lateral dimension up to larger sheets, both with conserved quality. As demonstrated on TMDs, and specifically MoS_2, SAW assisted exfoliation in dry condition gives a pristine quality exfoliated product of a desired thickness and lateral dimension, making the platform compatible with a variety of applications with little restrictions imposed. Therefore, the wide range of applications that has been found for exfoliated MoS_2, owing to its outstanding mechanical, electronic and optical properties, will not be limited by the synthesis technique. For example, in order to harness these unique properties for the benefit of biological application, the catalytic property of 2D MoS_2 can be of use in bioreactions as well as intercalation of organic entities and biological ions; both can be in turn basis of chemical sensing and photoluminescent biosensors for diagnostic purposes. When functionalization to bestow specificity to a target biomarker molecule is required, the introduction of defects, such as sulphur deficiencies exposing Mo atoms to functionalization or the exposed Mo the edges as well as the chalcogen atoms for disulphide bond formation. These modifications can be selectively introduced by design in a module added in succession to our non-invasive platform in a synthesis pipeline.